

Learning-Based Multi-Stage Strategy for a Fixed-Wing Aircraft to E evade a Missile Detected at a Short Distance

Zhiguan Niu

Xiaochao Zhou

Hao Xiong

Harbin Institute of Technology Shenzhen, China

Abstract— Missiles pose a major threat to aircraft in modern air combat. Advances in technology make them increasingly difficult to detect until they are close to the target and highly resistant to jamming. The evasion maneuver is the last line of defense for an aircraft. However, conventional rule-based evasion strategies are limited by computational demands and aerodynamic constraints, and existing learning-based approaches remain unconvincing for manned aircraft against modern missiles. To enhance aircraft survivability, this study investigates missile evasion inspired by the pursuit-evasion game between a gazelle and a cheetah and proposes a multi-stage reinforcement learning-based evasion strategy. The strategy learns a large azimuth policy to turn to evade, a small azimuth policy to keep moving away, and a short distance policy to perform agile aggressive maneuvers to avoid. One of the three policies is activated at each stage based on distance and azimuth. To evaluate performance, a high-fidelity simulation environment modeling an F-16 aircraft and missile under various conditions is used to compare the proposed approach with baseline strategies. Experimental results show that the proposed method achieves superior performance, enabling the F-16 aircraft to successfully avoid missiles with a probability of 80.89 percent for velocities ranging from 800 m/s to 1400 m/s, maximum overloads from 40 g to 50 g, detection distances from 5000 m to 15000 m, and random azimuths. When the missile is detected beyond 8000 m, the success ratio increases to 85.06 percent.

Index Terms— missile evasion, fixed-wing aircraft, reinforcement learning, multi-stage, short distance.

I. Introduction

Missiles pose a major threat to aircraft in modern air combat [1]–[3]. Missiles typically have much higher speed and superior maneuverability than their targets [4]. Advances in technology enable missiles to remain

Zhiguan Niu, Xiaochao Zhou, and Hao Xiong are with the School of Intelligence Science and Engineering, Harbin Institute of Technology Shenzhen, Shenzhen, China.

Corresponding author: Hao Xiong (e-mail: xionghao@hit.edu.cn).

undetected until they are close to the target. Due to their agility and the limited reaction and detection time available, missiles are increasingly difficult for pilots to evade [5]–[7]. During an evasion maneuver, pilots have only seconds to react while interpreting warning data and visually locating the threat [1]. Consequently, manual avoidance imposes a heavy cognitive workload and requires significant estimation, making real-time missile avoidance increasingly challenging for human pilots.

However, conventional missile avoidance techniques [8]–[11], such as programmed maneuvers and differential games, perform poorly [1] when an aircraft encounters a missile at close range. These methods are time-consuming [1] and often fail to accurately incorporate aircraft aerodynamics, which are critical for close-range avoidance [12]. Recent advances in reinforcement learning (RL) [13]–[15] provide a promising approach to enhance evasion maneuvers and improve pilot survivability. An RL-based evasion policy can learn to respond rapidly and precisely to an incoming missile, optimizing maneuvers according to the aircraft's state and performance.

Scholar have achieved amazing process is air combat [16]–[18] and pursuit-evasion game of the aircraft [19]–[21] based on RL in recent years. Also, scholar have also applied RL to address the missile evasion problem for aircraft. Narne et al. developed a real-time cooperative guidance strategy for an aircraft evading an incoming missile. The aircraft executes evasive maneuvers while launching a defensive missile to intercept or divert the attacker [22]. Liu et al. proposed a prediction-information-based twin delayed deep deterministic policy gradient decision-making algorithm for aircraft, enabling autonomous evasion against interceptor attacks in an adversarial environment [23]. Chen et al. proposed a Monte Carlo-based Deep Q-Network algorithm that integrates the Monte Carlo reinforcement learning framework with the DQN approach to address the evasion problem for high-speed aircraft [24]. Scukins et al. proposed a decision-support tool to assist pilots in Beyond Visual Range air combat by addressing the complexity of multiple missile threats [25]. Chen et al. developed a deep reinforcement learning-based evasion strategy for unpowered aircraft, achieving coordinated control of angle of attack, bank angle, and body morphing [26]. Ozbek proposed a reinforcement learning approach for generating real-time missile evasion maneuvers using the twin delayed deep deterministic policy gradient algorithm with a two-term reward function, and validated it using the Harfang simulator [27]. Li et al. developed a deep reinforcement learning-based maneuver evasion strategy to enhance an aircraft's autonomous capability to penetrate defended airspace [28]. Cook et al. focused on evading surface-to-air missiles and proposed using deep reinforcement learning to train a guidance policy that assumes control of the aircraft upon missile detection [4]. Yuan et al. investigated a hierarchical, goal-guided learning method enabling an aircraft to evade multiple missiles by detecting threats at long range [29]. Yan et

al. introduced a maneuvering strategy that combines line-of-sight (LOS) angle rate correction with RL to enable high-speed aircraft to evade pursuers [1]. Zhang et al. introduced a risk-sensitive PPO algorithm and a training framework incorporating multi-head attention and dual-population adversarial training to improve adaptability to various unknown missile types [5]. However, the above-mentioned studies have one or more limitations in the implementation details, reward function design, aircraft aerodynamics model, applicability to general scenarios, integration of the aircraft characteristics into the architecture and training of a strategy, statistical validation, or dependence on additional survival technologies (e.g., decoy).

This study is inspired by our previous research [12], which explored a method for aircraft based on RL to respond to dynamic obstacles within short distances. This study observes that 1) a missile can remain silent until it is at a short distance from the target and 2) the movement of a missile is insensitive to evasion maneuvers at a large distance but is sensitive to evasion maneuvers within a certain short distance. Thus, this study starts from addressing a missile at a short distance and then extends to addressing a missile at a farther distance. Based on the above work, this study proposes a multi-stage RL-based evasion strategy for an aircraft evading a missile at a short distance. The strategy is activated only upon detection of an approaching missile. In particular, this study focuses on a general mainstream air combat scenario of an aircraft encountering a missile. In such a scenario, a missile can have different velocities and maneuver capabilities that are considerably higher or better than those of the aircraft and come from a different direction. The aircraft can have a different velocity. A general scenario is challenging for the training of an effective RL-based evasion strategy and has not been comprehensively solved and validated in the above-mentioned references. Moreover, a multi-stage architecture and corresponding reward functions are designed based on the observations of multi-stage characteristic. Previous related studies have not utilized the characteristic to improve the architecture but usually apply a learning-based policy to address all possible states, making the training of a policy challenging.

The major contributions of this paper are as follows.

- A multi-stage RL-based strategy without requiring modification of an easy-to-use vanilla RL algorithm is developed for aircraft to address an approaching missile with different conditions at a short distance. Different from existing reinforcement learning-based evasion strategies, this study addresses a general scenario of an aircraft evading a missile through integrating insights of the multi-stage scenario into strategy architecture with corresponding reward functions, and includes detailed validation.
- Training and comparison experiments have been conducted in a close-to-real simulation environment of an F-16 aircraft based on the JSBSim simu-

lator and a numerical missile with conditions set according to realistic scenarios, accounting for the aerodynamics of the aircraft and the different maneuvering capabilities, velocities, incoming directions, and detected distance of the missile. Experimental results suggest that the multi-stage evasion strategy empowered by machine intelligence can considerably enhance the last line of defense for aircraft in modern air combat.

The remaining sections of this paper are structured as follows. Section II demonstrates the preliminaries of this study, including the problem statement and the notation for the scenario of an aircraft encountering a missile. Section III proposes a multi-stage RL-based evasion strategy for an aircraft to address an incoming missile at different distances. Section IV presents the details of the implementation and training of the multi-stage RL-based strategy and conducts comparative experiments based on the JSBSim simulator to demonstrate the effectiveness of the proposed multi-stage RL-based strategy. Finally, Section V summarizes the paper and suggests potential directions for future research.

II. Preliminaries

In this section, the problem statement and notations of the scenario of an aircraft evading a missile are introduced.

A. Problem statement

This study addresses a general scenario of an aircraft evading a missile, as shown in Fig. 1, to investigate and improve the survivability of the aircraft in an adversarial environment. In such a scenario, the aircraft can have a different initial velocity. The aircraft may encounter a missile incoming from different directions and observe the missile at an uncertain short distance. The missile can have a different velocity that is considerably larger than the velocity of the aircraft. The maneuvering capability of the missile, represented by maximum overload, is considerably larger than that of the aircraft. The missile tracks the aircraft according to a mainstream navigation law such as Proportional Navigation (PN) or Augmented Proportional Navigation (APN). It is assumed that the aircraft can observe the velocity and attitude of itself. Also, the aircraft can observe or estimate the position and velocity of a detected missile with respect to the aircraft with advanced devices.

B. Notations

The notations of the scenario of an aircraft encountering a missile are illustrated in Fig. 1. A world frame is defined to specify the state of the aircraft and the missile. This study defines the world frame based on the east-north-up (ENU) coordinate system. The positive directions of the x-axis, y-axis, and z-axis correspond to

east, north, and up, respectively. The origin of the world frame is located below the initial position of the aircraft and at sea level. The position of the aircraft is defined as $x_a = [x_a, y_a, z_a]$. The velocity of the aircraft is defined as $\dot{x}_a = [\dot{x}_a, \dot{y}_a, \dot{z}_a]$. The attitude of the aircraft is defined as $[\theta, \phi, \psi]$. The position of the missile with respect to the aircraft is defined as $\Delta x_m = [\Delta x_m, \Delta y_m, \Delta z_m]$. The velocity of the missile with respect to the aircraft is defined as $\Delta \dot{x}_m = [\Delta \dot{x}_m, \Delta \dot{y}_m, \Delta \dot{z}_m]$. The azimuth of the missile with respect to the aircraft is defined as Ψ based on the opposite direction of the heading of the aircraft. The azimuth is positive if the missile is on the right side and vice versa. The elevation of the missile with respect to the aircraft is defined as Θ . The elevation is positive if the missile is above the horizontal plane defined by the aircraft and vice versa.

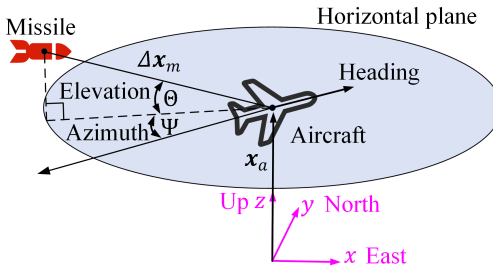


Fig. 1. Notations of the scenario of an aircraft evading a missile.

III. Method

In this section, a multi-stage RL-based strategy is developed for an aircraft to address a missile at a short distance. The multi-stage RL-based strategy is tailored for the scenario of an aircraft encountering a missile at a short distance from the perspectives of strategy architecture, reward functions, and training for generalization.

The multi-stage RL-based strategy has a multi-stage architecture, including a short distance stage, a relatively long distance and small azimuth stage, and a relatively long distance and large azimuth stage. The short distance stage aims to guide the aircraft to avoid the missile. The relatively long distance and small azimuth stage and relatively long distance and large azimuth stage aim to provide better conditions for the aircraft to avoid the missile in the short distance stage and postpone the start of the short distance stage to wear out the effective time of the missile.

The flow diagram of the multi-stage RL-based strategy is shown in Fig. 2. To achieve the multi-stage RL-based strategy, one should train a short distance policy for the short distance stage (detailed in Section III-A), and then analyze the performance of the short distance policy with different initial conditions (detailed in Section III-B). Based on the performance, one should determine the switching conditions that are beneficial for the short distance policy. According to the switching conditions, one should train a small azimuth policy (detailed in Section

III-C) and a large azimuth policy (detailed in Section III-D) for scenarios that do not satisfy the switching conditions. Eventually, the multi-stage RL-based strategy can be achieved by combining the three policies. The multi-stage RL-based strategy determines the stage based on the initial conditions of a scenario and switches to the activated policy according to Fig. 2.

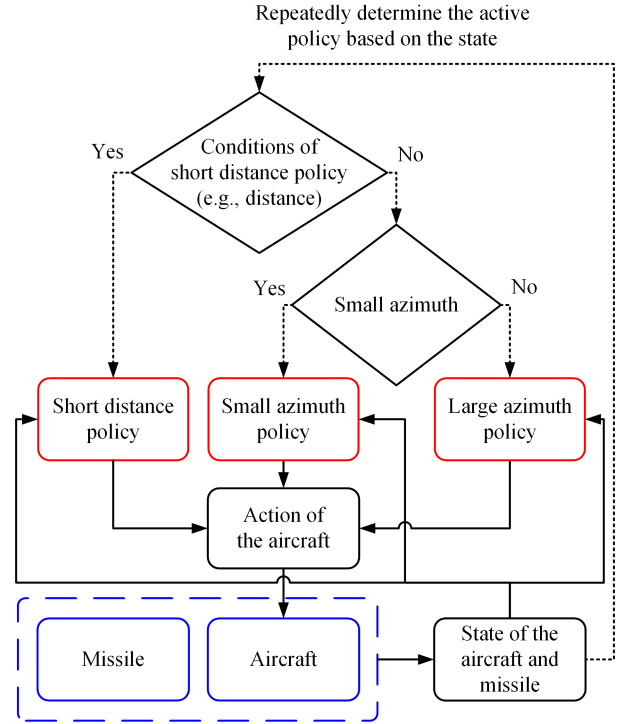


Fig. 2. Flow diagram of the multi-stage RL-based evasion strategy.

A. Short distance policy

The short distance policy is trained to increase the LOS of the missile, inspired by the PN law, and thus survive the aircraft. The short distance policy tends to guide the aircraft to perform large overload maneuvers when the missile is close to the aircraft, and thus force the missile to miss the aircraft due to the limit of the maximum overload. To make the short distance policy more trainable, this paper proposes to train a pretrain policy that makes the aircraft to perform large overload maneuvers (e.g., a steep turn policy), according to curriculum learning [30]. Then, based on the pretrain policy, it has a better chance of successfully training the short distance policy.

1. Steep turn policy

Steep turn is a common evasion maneuver [31]. One can obtain a steep turn policy as the pretrain policy for the short distance policy. The reward function of the steep turn policy can be expressed as

$$r_{\text{turn}} = \omega_{\text{turn}}^{\text{roll}} r_{\text{turn}}^{\text{roll}} + \omega_{\text{turn}}^{\text{pitch}} r_{\text{turn}}^{\text{pitch}} \quad (1)$$

where $r_{\text{turn}}^{\text{roll}}$ and $r_{\text{turn}}^{\text{pitch}}$ are the roll reward and pitch reward, respectively. $\omega_{\text{turn}}^{\text{roll}}$ and $\omega_{\text{turn}}^{\text{pitch}}$ are the corresponding weights of roll reward and pitch reward, respectively.

The roll reward $r_{\text{turn}}^{\text{roll}}$ guides the aircraft to perform a large roll angle to make a steep turn and can be expressed as

$$r_{\text{turn}}^{\text{roll}} = e^{-\frac{|\phi - \text{sgn}((\Delta\mathbf{x}_m \times \dot{\mathbf{x}}_a) \cdot \mathbf{u}_{\text{up}}) \cdot \phi^*|}{\tau_{\text{turn}}^{\text{roll}}}} \quad (2)$$

where ϕ denotes the roll of the aircraft and ϕ^* denotes the target roll. $\tau_{\text{turn}}^{\text{roll}}$ is an adjustable parameter. $\text{sgn}((\Delta\mathbf{x}_m \times \dot{\mathbf{x}}_a) \cdot \mathbf{u}_{\text{up}})$ determines a left or right turn based on the position of the missile with respect to the aircraft, represented by $\Delta\mathbf{x}_m$, and the velocity of the aircraft, represented by $\dot{\mathbf{x}}_a$. \mathbf{u}_{up} is the upward unit vector.

The pitch reward $r_{\text{turn}}^{\text{pitch}}$ tends to maintain the altitude of the aircraft and can be expressed as

$$r_{\text{turn}}^{\text{pitch}} = e^{-\frac{|\theta - \theta^*|}{\tau_{\text{turn}}^{\text{pitch}}}} \quad (3)$$

where θ^* denotes the target pitch for altitude keeping. $\tau_{\text{turn}}^{\text{pitch}}$ is an adjustable parameter.

2. Short distance policy

A short distance policy is trained based on the steep turn policy and the reward function with an additional LOS term. The reward function can be expressed as

$$r_{\text{short}} = \omega_{\text{turn}}^{\text{roll}} r_{\text{turn}}^{\text{roll}} + \omega_{\text{turn}}^{\text{pitch}} r_{\text{turn}}^{\text{pitch}} + \omega_{\text{short}}^{\text{LOS}} r_{\text{short}}^{\text{LOS}} \quad (4)$$

where $r_{\text{short}}^{\text{LOS}}$ is the LOS reward and $\omega_{\text{short}}^{\text{LOS}}$ is the corresponding weight of the LOS reward. This study proposes to learn a short distance policy that tends to avoid a missile by horizontal aggress maneuvers. In this way, the short distance policy is still applicable even if the altitude of the aircraft is not high. Thus, the LOS reward is designed based on the assumption that the pitch reward can guide the aircraft to maneuver in a horizontal plane roughly, and then $\Delta\mathbf{x}_m$ is approximately horizontal. $r_{\text{short}}^{\text{LOS}}$ can be expressed as

$$r_{\text{short}}^{\text{LOS}} = \tanh\left(\frac{\text{sgn}((\Delta\mathbf{x}_m \times \dot{\mathbf{x}}_a) \cdot \mathbf{u}_{\text{up}}) \cdot \dot{\lambda}^s}{\tau_{\text{short}}^{\text{LOS}}}\right) \quad (5)$$

$\text{sgn}((\Delta\mathbf{x}_m \times \dot{\mathbf{x}}_a) \cdot \mathbf{u}_{\text{up}})$ determines if the missile is on the left or right side of the aircraft, and has been included in (2) also. For instance, if a missile is on the right side of the aircraft, $\text{sgn}((\Delta\mathbf{x}_m \times \dot{\mathbf{x}}_a) \cdot \mathbf{u}_{\text{up}})$ is positive. $\tau_{\text{short}}^{\text{LOS}}$ is an adjustable parameter. $\dot{\lambda}^s$ is a signed LOS rate defined as

$$\dot{\lambda}^s = \text{sgn}((\mathbf{u}_m(t-1) \times \mathbf{u}_m(t)) \cdot \mathbf{u}_{\text{up}}) \cdot \frac{\|\mathbf{u}_m(t) - \mathbf{u}_m(t-1)\|}{\Delta t} \quad (6)$$

where $\mathbf{u}_m = \frac{\Delta\mathbf{x}_m}{\|\Delta\mathbf{x}_m\|}$ is the unit vector of the position of the missile with respect to the aircraft. For instance, if the aircraft make a missile on the right side and moving right further, $\text{sgn}((\mathbf{u}_m(t-1) \times \mathbf{u}_m(t)) \cdot \mathbf{u}_{\text{up}})$ is positive and thus the signed LOS rate is positive. It should be noted that this study proposes the signed LOS rate $\dot{\lambda}^s$ to guide the short distance policy to learn to increase the LOS of the missile

for the benefit of the aircraft, rather than maximizing the magnitude of the LOS rate according to [1], [32].

B. Policy switching

With different initial conditions, it is hard for the short distance policy to have the same performance in success ratio. The initial distance, the initial velocity and roll of the aircraft, the initial velocity of the missile, the initial azimuth of the missile etc. can make a big difference. This study proposes to investigate the performance of the short distance policy with different initial conditions, including but not limited to the above-mentioned conditions. The initial conditions that can lead to the best performance of the short distance policy should be the target of the small azimuth policy and large azimuth policy, as well as the conditions for switching from the small azimuth policy or large azimuth policy to the short distance policy.

C. Small azimuth policy

If the conditions of the short distance policy are not satisfied and the missile incomes from a small azimuth direction, the small azimuth policy will be activated and guide the aircraft to move away to wear out the effective time of the missile as possible and achieve beneficial conditions for the short distance policy. According to this study, the objectives of the small azimuth policy include (1) ensuring a small azimuth of the missile, (2) maintaining the altitude and attitude of the aircraft, (3) making the aircraft move in the opposite direction from the missile, and (4) accelerating the aircraft.

The reward function of the small azimuth policy can be expressed as

$$r_{\text{small}} = r_{\text{small}}^{\text{roll}} + r_{\text{small}}^{\text{pitch}} + r_{\text{small}}^{\text{azimuth}} + r_{\text{small}}^{\text{vel}} + c_{\text{small}}^{\text{roll}} + c_{\text{small}}^{\text{pitch}} + c_{\text{small}}^{\text{azimuth}} + c_{\text{small}}^{\text{vel}} \quad (7)$$

where $r_{\text{small}}^{\text{roll}}$ and $c_{\text{small}}^{\text{roll}}$ are the roll reward and the roll constraint, respectively. $r_{\text{small}}^{\text{pitch}}$ and $c_{\text{small}}^{\text{pitch}}$ can be expressed as

$$r_{\text{small}}^{\text{roll}} = e^{-\frac{|\phi|}{\tau_{\text{small}}^{\text{roll}}}} \quad (8)$$

$$c_{\text{small}}^{\text{roll}} = \begin{cases} P_{\text{small}}^{\text{roll}}, & \text{if } |\phi| > \phi_{\text{small}}^{\text{max}} \\ 0, & \text{otherwise} \end{cases} \quad (9)$$

where $\tau_{\text{small}}^{\text{roll}}$ is an adjustable parameter. $\phi_{\text{small}}^{\text{max}}$ denotes the upper boundary of the magnitude of roll set for the small azimuth policy. $P_{\text{small}}^{\text{roll}}$ is a negative constant as punishment.

$r_{\text{small}}^{\text{pitch}}$ and $c_{\text{small}}^{\text{pitch}}$ are the pitch reward and the pitch constraint, respectively. $r_{\text{small}}^{\text{pitch}}$ and $c_{\text{small}}^{\text{pitch}}$ can be expressed as

$$r_{\text{small}}^{\text{pitch}} = e^{-\frac{|\theta - \theta^*|}{\tau_{\text{small}}^{\text{pitch}}}} \quad (10)$$

$$c_{\text{small}}^{\text{pitch}} = \begin{cases} P_{\text{small}}^{\text{pitch}}, & \text{if } |\theta| > \theta_{\text{small}}^{\text{max}} \\ 0, & \text{otherwise} \end{cases} \quad (11)$$

where $\tau_{\text{small}}^{\text{pitch}}$ is an adjustable parameter. $\theta_{\text{small}}^{\text{max}}$ denotes the upper boundary of the magnitude of pitch set for the small azimuth policy. $P_{\text{small}}^{\text{pitch}}$ is a negative constant as punishment.

$r_{\text{small}}^{\text{azimuth}}$ and $c_{\text{small}}^{\text{azimuth}}$ are the azimuth reward and the azimuth constraint, respectively. $r_{\text{small}}^{\text{azimuth}}$ and $c_{\text{small}}^{\text{azimuth}}$ can be expressed as

$$r_{\text{small}}^{\text{azimuth}} = e^{-\frac{|\Psi|}{\tau_{\text{small}}^{\text{azimuth}}}} \quad (12)$$

$$c_{\text{small}}^{\text{azimuth}} = \begin{cases} P_{\text{small}}^{\text{azimuth}}, & \text{if } |\Psi| > \Psi_{\text{small}}^{\text{max}} \\ 0, & \text{otherwise} \end{cases} \quad (13)$$

where Ψ denotes the azimuth of the missile. $\tau_{\text{small}}^{\text{azimuth}}$ is an adjustable parameter. $\Psi_{\text{small}}^{\text{max}}$ represents the upper boundary of the magnitude of azimuth set for the small azimuth policy. $P_{\text{small}}^{\text{azimuth}}$ denotes a negative constant as punishment.

$r_{\text{small}}^{\text{vel}}$ and $c_{\text{small}}^{\text{vel}}$ are the velocity reward and the velocity constraint, respectively. $r_{\text{small}}^{\text{vel}}$ and $c_{\text{small}}^{\text{vel}}$ can be expressed as

$$r_{\text{small}}^{\text{vel}} = \tanh\left(\frac{\|\dot{\mathbf{x}}_a\| - \dot{x}_a^{\text{ref}}}{\tau_{\text{small}}^{\text{vel}}}\right) \quad (14)$$

$$c_{\text{small}}^{\text{vel}} = \begin{cases} P_{\text{small}}^{\text{vel}}, & \text{if } \|\dot{\mathbf{x}}_a\| > \dot{x}_a^{\text{max}} \text{ or } \|\dot{\mathbf{x}}_a\| < \dot{x}_a^{\text{min}} \\ 0, & \text{otherwise} \end{cases} \quad (15)$$

where $\dot{\mathbf{x}}_a$ denotes the velocity of the aircraft. \dot{x}_a^{ref} denotes a reference velocity used to adjust the effective range of \tanh . \dot{x}_a^{max} and \dot{x}_a^{min} denote the upper and lower boundaries of the aircraft, respectively. $P_{\text{small}}^{\text{vel}}$ is a negative constant as punishment.

D. Large azimuth policy

If the conditions of the short distance policy are not satisfied and the missile comes from a large azimuth direction, the large azimuth policy will be activated and guide the aircraft to turn to the opposite direction from the missile for moving away and achieve beneficial conditions for the short distance policy. If the large azimuth policy makes the aircraft achieve a small azimuth and the conditions of the short distance policy are not satisfied, the large azimuth policy will switch to the small azimuth policy. If the conditions of the short distance policy are satisfied, the large azimuth policy will switch to the short distance policy.

According to this study, the objectives of the large azimuth policy include (1) reducing the azimuth of the missile, (2) maintaining the altitude of the aircraft, (3) reducing the roll of the aircraft to around 0 deg quickly if the distance condition of the short distance policy is about to be satisfied, and (4) accelerating the aircraft.

The reward function of the large azimuth policy can be expressed as

$$r_{\text{large}} = r_{\text{large}}^{\text{roll}} + r_{\text{large}}^{\text{pitch}} + r_{\text{large}}^{\text{vel}} + c_{\text{large}}^{\text{roll}} + c_{\text{large}}^{\text{pitch}} + c_{\text{large}}^{\text{vel}} \quad (16)$$

where $r_{\text{large}}^{\text{roll}}$ and $c_{\text{large}}^{\text{roll}}$ are the roll reward and the roll constraint, respectively. $r_{\text{large}}^{\text{roll}}$ can be expressed as

$$r_{\text{large}}^{\text{roll}} = \begin{cases} r_{\text{large}}^{\text{far}}, & \|\Delta\mathbf{x}_m\| > d_c \\ r_{\text{large}}^{\text{close}}, & \|\Delta\mathbf{x}_m\| \leq d_c \end{cases} \quad (17)$$

where d_c is a critical distance. If the distance between the aircraft and the missile is larger than the critical distance (i.e., $\|\Delta\mathbf{x}_m\| > d_c$), the roll reward is

$$r_{\text{large}}^{\text{far}} = e^{-\frac{|\phi - \text{sgn}((\Delta\mathbf{x}_m \times \dot{\mathbf{x}}_a) \cdot \mathbf{u}_{\text{up}}) \cdot \phi^*|}{\tau_{\text{large}}^{\text{far}}}} \quad (18)$$

where ϕ^* denotes the target roll. $\tau_{\text{large}}^{\text{far}}$ is an adjustable parameter. If the distance between the aircraft and the missile is smaller than the critical distance (i.e., $\|\Delta\mathbf{x}_m\| \leq d_c$), the roll reward is given by

$$r_{\text{large}}^{\text{close}} = \begin{cases} P_{\text{large}}^{\text{roll}}, & |\phi| > \phi_{\text{large}}^{\text{short}} \\ R_{\text{large}}^{\text{roll}}, & |\phi| \leq \phi_{\text{large}}^{\text{short}} \end{cases} \quad (19)$$

where $\phi_{\text{large}}^{\text{short}}$ represents the upper boundary of the magnitude of roll set for reducing the roll of the aircraft to achieve a beneficial roll condition for the short distance policy. $P_{\text{large}}^{\text{roll}}$ is a negative constant as punishment. $R_{\text{large}}^{\text{roll}}$ is a positive constant as a reward. The roll constraint $c_{\text{large}}^{\text{roll}}$ can be expressed as

$$c_{\text{large}}^{\text{roll}} = \begin{cases} P_{\text{large}}^{\text{roll}}, & \text{if } |\phi| > \phi_{\text{large}}^{\text{max}} \\ 0, & \text{otherwise} \end{cases} \quad (20)$$

$\phi_{\text{large}}^{\text{max}}$ denotes the upper boundary of the magnitude of roll set for the large azimuth policy.

$r_{\text{large}}^{\text{pitch}}$ and $c_{\text{large}}^{\text{pitch}}$ are the pitch reward and the pitch constraint, respectively. $r_{\text{large}}^{\text{pitch}}$ and $c_{\text{large}}^{\text{pitch}}$ can be expressed as

$$r_{\text{large}}^{\text{pitch}} = e^{-\frac{|\theta - \theta^*|}{\tau_{\text{large}}^{\text{pitch}}}} \quad (21)$$

$$c_{\text{large}}^{\text{pitch}} = \begin{cases} P_{\text{large}}^{\text{pitch}}, & \text{if } |\theta| > \theta_{\text{large}}^{\text{max}} \\ 0, & \text{otherwise} \end{cases} \quad (22)$$

where $\theta_{\text{large}}^{\text{max}}$ denotes the upper boundary of the magnitude of pitch set for the large azimuth policy. $\tau_{\text{large}}^{\text{pitch}}$ is an adjustable parameter. $P_{\text{large}}^{\text{pitch}}$ is a negative constant as punishment.

$r_{\text{large}}^{\text{vel}}$ and $c_{\text{large}}^{\text{vel}}$ are the velocity reward and the velocity constraint, respectively. $r_{\text{large}}^{\text{vel}}$ and $c_{\text{large}}^{\text{vel}}$ can be expressed as

$$r_{\text{large}}^{\text{vel}} = \tanh\left(\frac{\|\dot{\mathbf{x}}_a\| - \dot{x}_a^{\text{ref}}}{\tau_{\text{large}}^{\text{vel}}}\right) \quad (23)$$

$$c_{\text{large}}^{\text{vel}} = \begin{cases} P_{\text{large}}^{\text{vel}}, & \text{if } \|\dot{\mathbf{x}}_a\| > \dot{x}_a^{\text{max}} \text{ or } \|\dot{\mathbf{x}}_a\| < \dot{x}_a^{\text{min}} \\ 0, & \text{otherwise} \end{cases} \quad (24)$$

where $\tau_{\text{large}}^{\text{vel}}$ is an adjustable parameter. $P_{\text{large}}^{\text{vel}}$ is a negative constant as punishment.

IV. Experiments

To evaluate the effectiveness of the developed evasion strategy in addressing a missile, close-to-real experiments are conducted. The experiments include the training and analysis of the three policies of the proposed evasion strategy, the training of a baseline RL-based evasion strategy, comparison of the proposed evasion strategy and existing evasion strategies, and tests of the proposed evasion strategy in addressing different navigation laws.

A personal computer with a 3.7 GHz CPU, 32 GB memory, and an RTX 3080 Ti GPU is used to conduct the experiments. This study runs the simulator at a frequency of 200 Hz to improve simulation accuracy. The aircraft is simulated based on the JSBSim simulator with the F-16 aircraft model [33]. The JSBSim simulator is a flight simulator that covers the aircraft's physical characteristics, aerodynamic model, flight control systems, and propulsion, and has been used in several academic studies [18], [25], [34]. To unleash maximum maneuver capability without being limited by a flight controller, the control inputs are designed to act on the elevator, aileron, rudder, and throttle of the aircraft.

This study simulates the movement of a missile in three-dimensional space. A horizontal navigation law and a vertical navigation law (e.g., a PN law) are designed for the missile inspired by [8]. The PN law can be expressed as

$$a_m = N \cdot V_c \cdot \dot{\lambda} \quad (25)$$

where a_m is a missile commanded acceleration. N is a navigation coefficient. V_c is the closing velocity between the missile and the aircraft, $\dot{\lambda}$ is the LOS rate. The yaw and pitch of the missile are updated according to the horizontal navigation law and a vertical navigation law in discrete form, inspired by [35]. The change of the yaw and pitch of the missile will be truncated proportionally, if the required overload is larger than the defined maximum overload of the missile. Then, the position of the missile is updated based on the yaw, pitch, and velocity of the missile in discrete form, according to [36].

A. Experiment setups

To simulate real-world scenarios of an aircraft evading a missile at a short distance, parameters are set for the scenarios in training and testing according to real parameters or references. The initial velocity of the aircraft ranges from 280 m/s to 470 m/s. [37], [38]. The initial altitude of the aircraft is set to range from 3000 m to 9000 m, inspired by the operational ceiling [39]. The minimum altitude of the aircraft is set to 1000 m. The initial heading of the aircraft is set between 0 deg and 360 deg.

A missile is set to approach the aircraft from an arbitrary horizontal direction. The initial azimuth of the missile ranges from -180 deg to 180 deg randomly. It should be emphasized that the azimuth of the missile with respect to the aircraft is defined based on the opposite direction of the heading of the aircraft. The

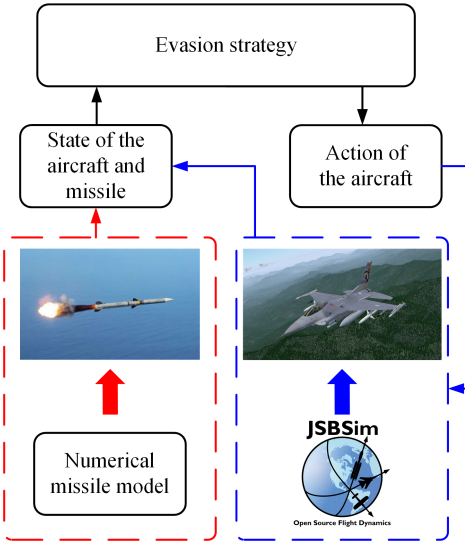


Fig. 3. Framework of simulation based on the JSBSim simulator.

TABLE I
Conditions of the scenarios investigated in the experiments

Parameter	Value
Initial altitude of the aircraft	3000 m to 9000 m
Initial velocity of the aircraft	280 m/s to 470 m/s
Initial heading of the aircraft	0 deg to 360 deg
Initial azimuth of the missile	-180 deg to 180 deg
Initial elevation of the missile	-15 deg to 15 deg
Initial distance	5000 m to 15000 m
Constant velocity of the missile	800 m/s to 1400 m/s
Maximum overload of the missile	40 g to 50 g
Lethal radius of the missile	10 m
Maximum duration	25 s

initial elevation of the missile ranges from -15 deg to 15 deg in the initial state. The initial distance between the aircraft and the missile is set within the range of 5–15 km to simulate a short distance scenario, inspired by [40]–[43]. The velocity of the missile ranges from 800 m/s and 1400 m/s according to [35], [44]. The velocity of the missile is set to be constant, aiming to achieve an evasion strategy that can address a challenging missile with the dual pulse technique. The maximum overload of the missile ranges from 40 g to 50 g according to [29], [32], [45]. Unless otherwise specified, the missile tracks the aircraft following the PN law [35], with the navigation coefficient randomly ranging from 3 and 5 according to [41]. The maximum duration of a scenario is set to 25 s based on the operation time of a missile [36]. The lethal zone of the missile is assumed to be a spherical region with a radius of 10 m [1], [40].

Table I lists the conditions of the scenarios discussed in the experiments.

B. Implementation of the multi-stage RL-based strategy

This study applies the multi-stage RL-based evasion strategy to address a general scenario of an aircraft evading a missile, specified in Section IV-A. The implementation of the multi-stage RL-based evasion strategy is demonstrated in this section. According to the multi-stage RL-based evasion strategy, this study first learns a short distance policy to address a missile that approaches the aircraft to a certain short distance. The training of short distance policy is specified in Section IV-C. Then, the performance of the short distance policy is investigated thoroughly in Section IV-D. Based on the performance, this study determines that the short distance policy is activated if the distance between the aircraft and the missile is less than 8000 m. The conditions that are beneficial for the short distance policy are determined and set as the objectives of the training of a small azimuth policy and a large azimuth policy. The beneficial conditions include a high velocity and a small roll of the aircraft. Next, this study set a threshold of 30 deg for the magnitude of the azimuth, and the training of a small azimuth policy and a large azimuth policy is specified in Section IV-E and Section IV-F, respectively. The multi-stage RL-based evasion strategy implemented in the experiments can be expressed as Fig. 4.

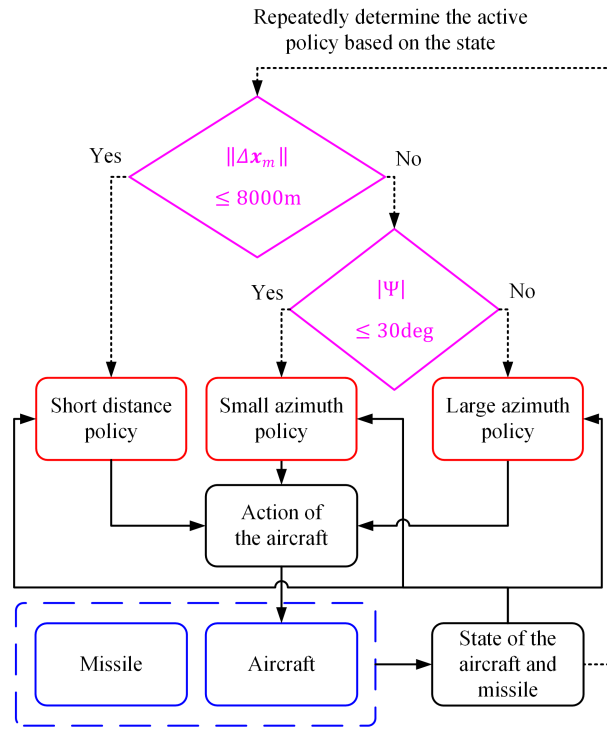


Fig. 4. Flow diagram of the obtained multi-stage RL-based evasion strategy.

The Proximal Policy Optimization (PPO) algorithm is used to train the three policies. A policy based on the PPO algorithm has an actor network and a critic network. In this study, both the actor network and critic network have two hidden layers with 256 units. Tanh is used as the

TABLE II
Feasible range of the state space and action space

Parameter	Lower bound	Upper bound
x element of the velocity of the aircraft \dot{x}_a	-470 m/s	470 m/s
y element of the velocity of the aircraft \dot{y}_a	-470 m/s	470 m/s
z element of the velocity of the aircraft \dot{z}_a	-470 m/s	470 m/s
Roll of the aircraft ϕ	-180 deg	180 deg
Pitch of the aircraft θ	-90 deg	90 deg
Heading of the aircraft ψ	0 deg	360 deg
x element of the position of the missile with respect to the aircraft Δx_m	-15000 m	15000 m
y element of the position of the missile with respect to the aircraft Δy_m	-15000 m	15000 m
z element of the position of the missile with respect to the aircraft Δz_m	-15000 m	15000 m
x element of the velocity of the missile with respect to the aircraft $\Delta \dot{x}_m$	-1870 m/s	1870 m/s
y element of the velocity of the missile with respect to the aircraft $\Delta \dot{y}_m$	-1870 m/s	1870 m/s
z element of the velocity of the missile with respect to the aircraft $\Delta \dot{z}_m$	-1870 m/s	1870 m/s
Control input on elevator δ_e	-1	1
Control input on aileron δ_a	-1	1
Control input on rudder δ_r	-1	1
Control input on throttle δ_t	0	1

activation function for all hidden layers and the output layer. The Adam optimizer is used for training.

According to the problem statement and experiment setting, the state space of a policy is set to $s = [\dot{x}_a, \dot{y}_a, \dot{z}_a, \theta, \phi, \psi, \Delta x_m, \Delta y_m, \Delta z_m, \Delta \dot{x}_m, \Delta \dot{y}_m, \Delta \dot{z}_m]$, where $[\dot{x}_a, \dot{y}_a, \dot{z}_a]$ reflects the velocity of the aircraft. $[\theta, \phi, \psi]$ denotes the roll, pitch, and heading of the aircraft. $[\Delta x_m, \Delta y_m, \Delta z_m]$ and $[\Delta \dot{x}_m, \Delta \dot{y}_m, \Delta \dot{z}_m]$ are the position and velocity of the missile with respect to the aircraft, respectively. According to the experiment setting, the action space of a policy is set to $a = [\delta_e, \delta_a, \delta_r, \delta_t]$. $[\delta_e, \delta_a, \delta_r, \delta_t]$ denotes normalized control inputs on the elevator, aileron, rudder, and throttle, respectively. Table II lists the upper and lower bounds of the state space and action space. The other hyperparameters used in this study are listed in Table III.

C. Training and validation of a short distance policy

This study applies the curriculum learning technique to make a short-distance policy more trainable. Since the short-distance policy needs to perform agile and

TABLE III
Hyperparameters used in the training of policies

Hyperparameter	Value
Discount factor	0.99
Learning rate	3×10^{-4}
Maximum number of steps	7500
Batch size	1024

aggressive maneuvers to evade a missile, the training of the short-distance policy includes two phases - 1) training a steep turn policy and 2) training a short-distance policy based on the steep turn policy.

In both phases, scenarios with the same setting listed in Table I are adopted. The initial position of the aircraft is set to $[0, 0, z_a]$ (unit: m), where z_a represents an altitude randomly selected from 3000 m to 9000 m. The initial heading of the aircraft is randomly set ranging from 0 deg to 360 deg. Both the initial roll and pitch of the aircraft are set to 0 deg. The initial velocity of the aircraft is randomly selected from 280 m/s to 470 m/s.

According to preliminary tests, it is shown that aggressive evasion maneuvers of the aircraft are less effective, if the distance between the aircraft and the missile is larger than 12000 m. Thus, this study trains a short distance policy focusing on distance ranging from 5000 m to 12000 m, and thus the missile is set to have a random distance of 5000 m to 12000 m from the aircraft. The azimuth of the missile is random. The elevation of the missile randomly ranges from -15 deg to 15 deg. The velocity of the missile is a constant ranging from 800 m/s to 1400 m/s. The maximum overload of the missile is randomly selected from 40 g to 50 g. The missile follows the PN law with a randomly selected navigation coefficient ranging from 3 to 5. The maximum number of steps of an episode is 7500. An episode will be terminated if the aircraft is caught by the missile.

1. Steep turn policy

Training. This study learns a steep turn policy through training the policy to make an aircraft keep performing a large roll. The target angle is set to 85 deg. The target pitch is set to 0 deg to avoid losing too much altitude. According to (1), the reward function of the steep turn policy is defined as

$$r_{\text{turn}} = 0.5e^{-\frac{|\phi - \text{sgn}((\Delta\mathbf{x}_m \times \dot{\mathbf{x}}_a) \cdot \mathbf{u}_{\text{up}}) \cdot 85|}{0.2}} + 0.5e^{-\frac{|\theta|}{0.2}} \quad (26)$$

The learning process of the steep turn policy can be reflected by the achieved reward presented in Fig. 5. The learning process converges in 3000 episodes.

Validation. To validate the performance of the learned steep turn policy, a test is performed. The test is set to have a maximum number of 5000 steps (i.e., 25 s) and the missile is set to 21000 m from the aircraft, so as to enable

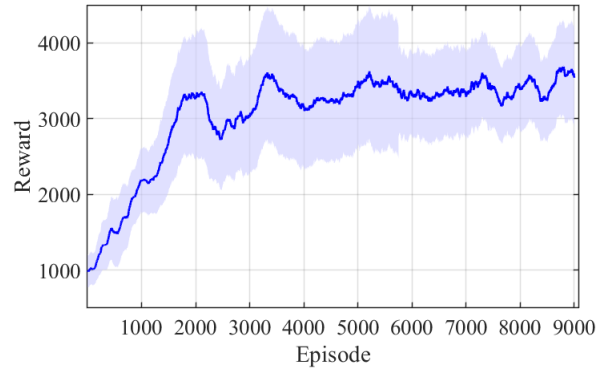


Fig. 5. Accumulated reward achieved in the training of a steep turn policy.

the aircraft to finish a circle trajectory. If the position of the missile $\Delta\mathbf{x}_m$ is beyond the state space, the position will be truncated.

In the initial of the test, the position of the aircraft is set to $[0, 0, 5097]$ (unit: m). The heading of the aircraft is set to 0 deg. Both the roll and pitch of the aircraft are set to 0 deg. The initial velocity of the aircraft is set to 280 m/s. The aircraft follows the learned steep turn policy. The initial missile is 21000 m from the aircraft. The initial azimuth of the missile is 0 deg (i.e., behind the aircraft). The initial elevation of the missile is -6.27 deg. The velocity of the missile is constantly 800 m/s. The maximum overload of the missile is randomly set to 42.97 g. The missile follows the PN law with a randomly selected navigation coefficient of 3.82.

Fig. 6 shows the trajectory of the aircraft and the missile. Fig. 7 and Fig. 8 show the roll and pitch angle of the aircraft. It is shown that the roll of the aircraft is around 85 deg and the pitch of the aircraft is about 0 deg. The learned steep turn policy can guide the aircraft to perform a circle trajectory. The effectiveness of the steep turn policy is verified.

2. Short distance policy

Training. A PN law determines a reference lateral acceleration proportional to LOS rate to chase a target [46]. The PN law inspires this study to design a reward term based on the LOS rate for the short distance policy. Based on the reward function of the steep turn policy 26, the reward function of the short distance policy is defined as

$$r_{\text{short}} = 0.5e^{-\frac{|\phi - \text{sgn}((\Delta\mathbf{x}_m \times \dot{\mathbf{x}}_a) \cdot \mathbf{u}_{\text{up}}) \cdot 85|}{0.2}} + 0.5e^{-\frac{|\theta|}{0.2}} + 0.6 \tanh\left(\frac{\text{sgn}((\Delta\mathbf{x}_m \times \dot{\mathbf{x}}_a) \cdot \mathbf{u}_{\text{up}}) \cdot \dot{\lambda}^s}{0.1}\right) \quad (27)$$

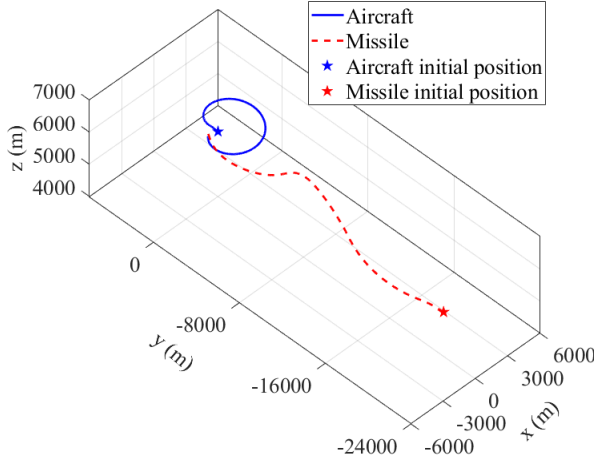


Fig. 6. Trajectory of the aircraft and the missile in the test of the steep turn policy.

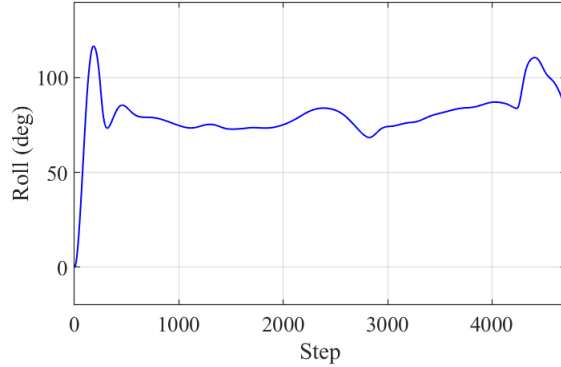


Fig. 7. Roll of the aircraft in the test of the steep turn policy.

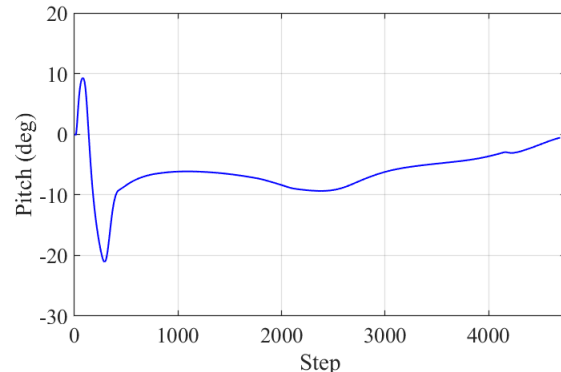


Fig. 8. Pitch of the aircraft in the test of the steep turn policy.

Since the simulation frequency is 200 Hz, leading to a fluctuating LOS rate, this study smooths $\dot{\lambda}$ by

$$\dot{\lambda}^s(t) = 0.25\dot{\lambda}_{\text{raw}}^s(t) + 0.75\dot{\lambda}^s(t-1) \quad (28)$$

where $\dot{\lambda}_{\text{raw}}^s(t)$ is the raw value of the signed LOS rate at step t .

The learning process of the short distance policy can be reflected by the achieved reward presented in Fig. 9. The learning process converges in 4000 episodes.

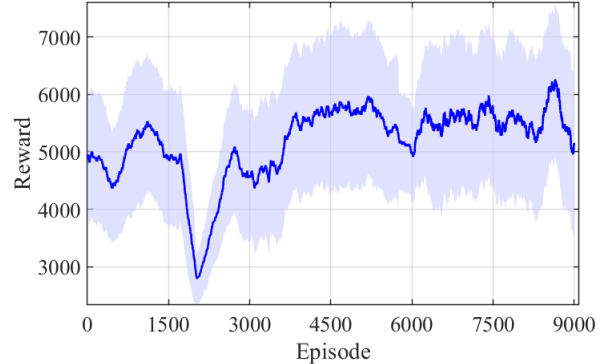


Fig. 9. Accumulated reward achieved in the training of the short distance policy.

Validation. To evaluate the performance of the short distance policy, a test is performed. The test is set to have a maximum number of 5000 steps (i.e., 25 s). In the initial of the test, the position of the aircraft is set to [0, 0, 4820] (unit: m). The heading of the aircraft is set to 0 deg. Both the roll and pitch of the aircraft are set to 0 deg. The velocity of the aircraft is set to 280 m/s. The aircraft follows the short distance policy. The missile is 6000 m from the aircraft. The azimuth of the missile is 30 deg. The elevation of the missile is -3.41 deg. The velocity of the missile is 800 m/s. The maximum overload of the missile is randomly set to 46.92 g. The missile follows the PN law with a randomly selected navigation coefficient of 4.17.

Fig. 10 shows the trajectory of the aircraft and the missile. Fig. 11 shows rewards corresponding to the roll and pitch of the aircraft and LOS rate. It is shown that the short distance policy can balance the objectives in controlling the roll and pitch, and increasing the LOS rate, since the magnitude of the rewards is comparable. Fig. 12, Fig. 13, and Fig. 14 show the roll and pitch of the aircraft and LOS rate. The overload of the aircraft and the missile is shown in Fig. 15. When the missile is close to the aircraft, the overload of the missile increases sharply. Fig. 16 shows the distance between the aircraft and the missile. According to the figures, one can see that the short distance policy can maintain the roll and pitch under control (Fig. 12 and Fig. 13) and considerably increase the LOS rate when the missile is close to the aircraft (Fig. 14) and maximize the overload of the missile (Fig. 15). As a result, the short distance policy enable the aircraft to successfully avoid the missile (Fig. 10).

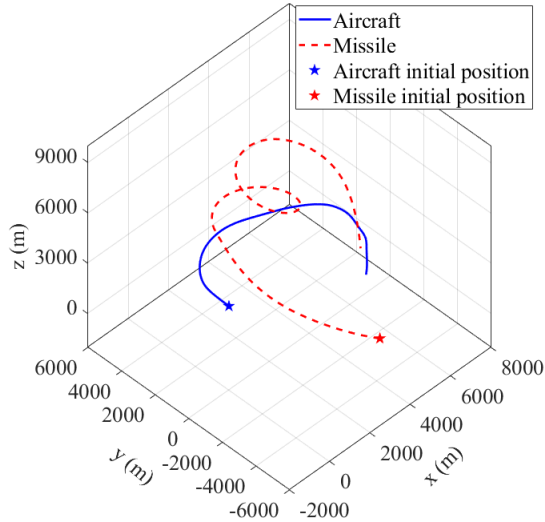


Fig. 10. Trajectory of the aircraft and the missile in the test of the short distance policy.

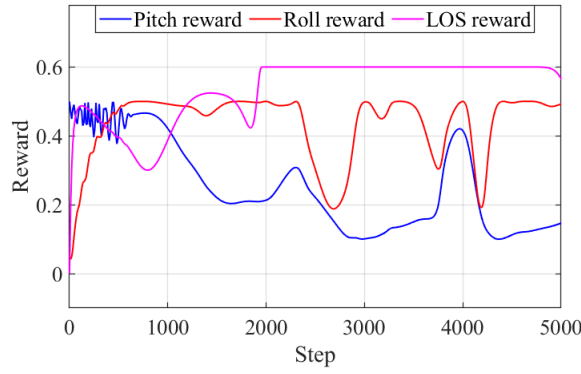


Fig. 11. Itemized rewards per step calculated based on the state of the aircraft and the missile in the test of the short distance policy.

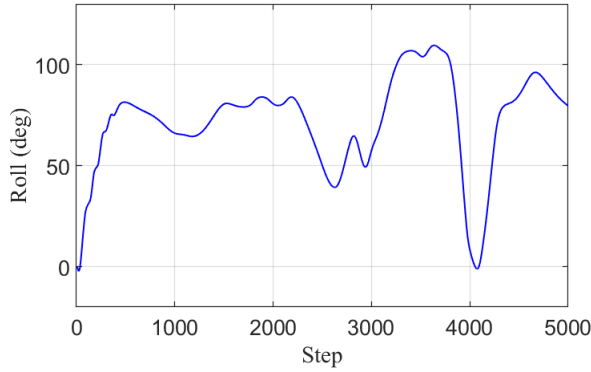


Fig. 12. Roll of the aircraft in the test of the short distance policy.

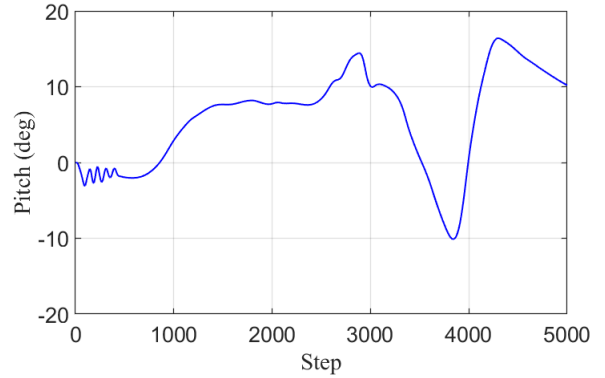


Fig. 13. Pitch of the aircraft in the test of the short distance policy.

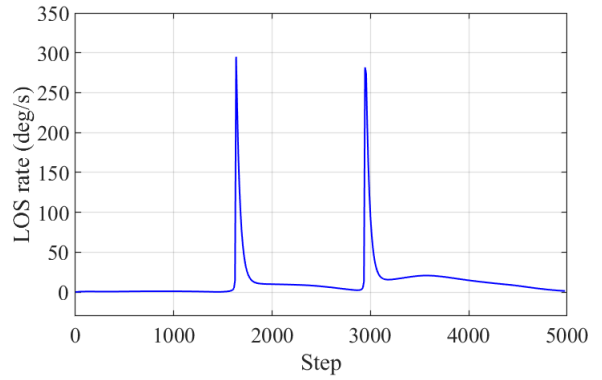


Fig. 14. LOS rate in the test of the short distance policy

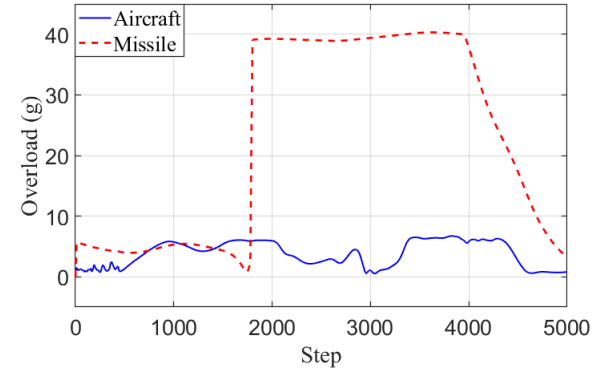


Fig. 15. Overload of the aircraft and the missile in the test of the short distance policy.

D. Determination of the conditions of policy switching

According to the proposed multi-stage RL-based policy, one should investigate the short distance policy and determine the beneficial conditions for switching to the short distance policy. To investigate the short-distance

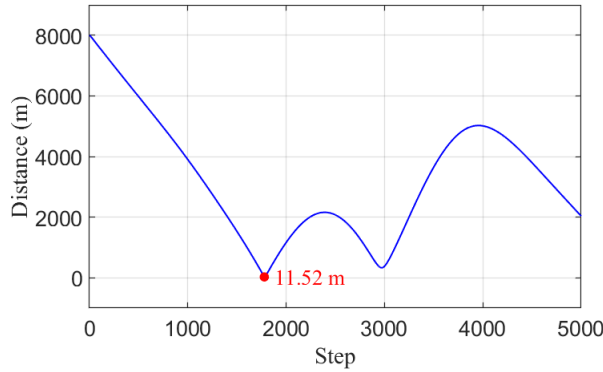


Fig. 16. Distance between the aircraft and the missile in the test of the short distance policy.

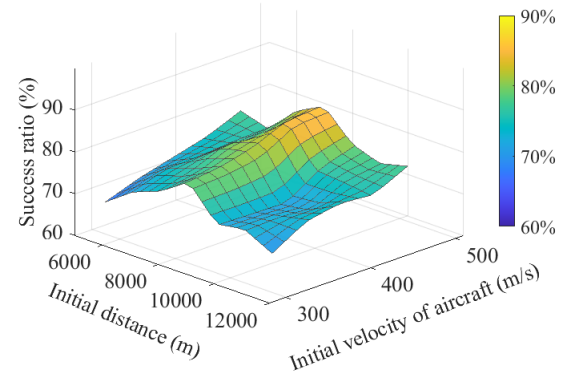


Fig. 17. Success ratio of the short distance policy with different initial conditions.

policy, a statistical analysis is conducted through dividing the initial conditions of the aircraft and the missile into intervals and then performing tests. The maximum number of steps of a test is 5000 (i.e., 25 s). (1) The initial velocity of the aircraft is divided into intervals ranging from 280 m/s to 470 m/s, with a step of 40 m/s. (2) The initial velocity of the missile is divided into intervals ranging from 800 m/s and 1400 m/s, with a step of 100 m/s. (3) The initial distance between the aircraft and the missile is divided into intervals ranging from 5000 m to 12000 m, with a step of 1000 m. (4) The initial azimuth of the missile is divided into intervals ranging from -180 deg to 180 deg, with a step of 30 deg. The initial roll and pitch of the aircraft are set to 0 deg. The other initial conditions are randomly selected, according to Table I. The missile follows the PN law with a randomly selected navigation coefficient ranging from 3 to 5.

For an interval determined by the initial velocities of the aircraft and the missile, the initial distance between the aircraft and the missile, and the initial azimuth of the missile, the other initial conditions are randomly selected and 40 tests have been conducted. The success ratio achieved by the short-distance policy is calculated to investigate the performance, as shown in Fig. 17.

The experimental results indicate that the best success ratio is achieved if the initial distance is around 8000 m to 9000 m. Moreover, the increase of the velocity of the aircraft increases the success ratio. According to the experimental results, this study involves the distance of 8000 m as one of the conditions of switching to the short distance policy and set accelerating the aircraft as an objective for the small azimuth policy and the large azimuth policy.

It should be noticed that the performance of the short-distance policy in addressing a long initial distance scenario is not as good as the performance in addressing an 8000 m initial distance scenario. This result is not reasonable, since if an aircraft with a long initial distance from a missile maintains level flight and then switch to the

short-distance policy at 8000 m distance, the aircraft can achieve the same performance in addressing an 8000 m initial distance scenario. To investigate the unreasonable result, another statistical analysis is conducted to disclose the difference between the state of an aircraft with an 8000 m initial distance and the state of an aircraft when the distance decrease from 12000 m to 8000 m following the short-distance policy. The statistical analysis divides the initial conditions of the aircraft and the missile into intervals and initializes the other initial conditions in the same way as the statistical analysis corresponding to Fig. 17, except for the 12000 m initial distance. The maximum number of steps of a test is 5000 (i.e., 25 s). For an interval determined by the initial velocities of the aircraft and the missile, and the initial azimuth of the missile, 5 tests have been conducted. It is shown that if an aircraft starts to follow the short distance policy at an initial distance of 12000 m, the roll of the aircraft is approximately 85 deg or -85 deg when the distance is decreased by the missile to 8000 m, as shown in Fig. 18. The major difference between the state of an aircraft with an 8000 m initial distance and the state of an aircraft when the distance decrease from 12000 m to 8000 m is the roll of the aircraft.

To evaluate the influence of the initial roll of the aircraft on the success ratio, a statistical analysis is conducted to disclose the success ratio of an aircraft with an 8000 m initial distance but with different roll angles. The statistical analysis divides the initial conditions of the aircraft and the missile into intervals and initializes the other initial conditions in the same way as the statistical analysis corresponding to Fig. 17, except for the 8000 m initial distance and different initial roll angles of -85 deg, 0 deg, and 85 deg. The maximum number of steps of a test is 5000 (i.e., 25 s). For an interval determined by the initial velocities of the aircraft and the missile, the initial azimuth of the missile, and the roll of the aircraft, 5 tests have been conducted. The result of the influence of the initial roll of the aircraft on the success

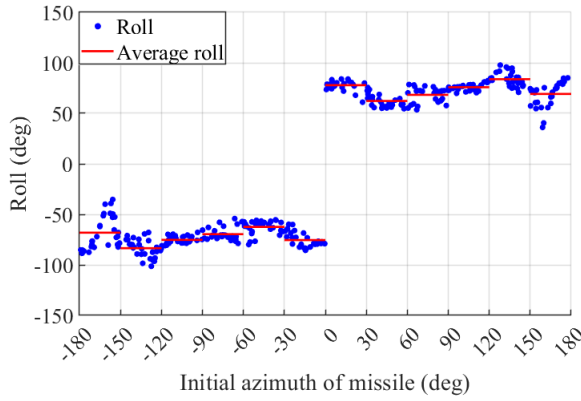


Fig. 18. Roll of the aircraft at a distance of 8000 m following the short distance policy to address a missile initialized at a distance of 12000 coming from different directions.

ratio is shown in Fig. 19. The result indicates that for an aircraft with an 8000 m initial distance, the 0 deg roll in the initial state can provide a considerably higher success ratio than a large roll (e.g., -85 deg or 85 deg) in the initial state. According to the experimental result, this study set reducing the roll of the aircraft to about 0 deg when switching to the short distance policy as an objective for the small azimuth policy and the large azimuth policy.

Remark 1. According to the analysis of the short distance policy in this section, 1) the condition of switching to the short distance policy is the distance of 8000 m and the objectives of the small azimuth policy and the large azimuth policy include 2) accelerating the aircraft and 3) reducing the roll of the aircraft to around 0 deg when switching to the short distance policy.

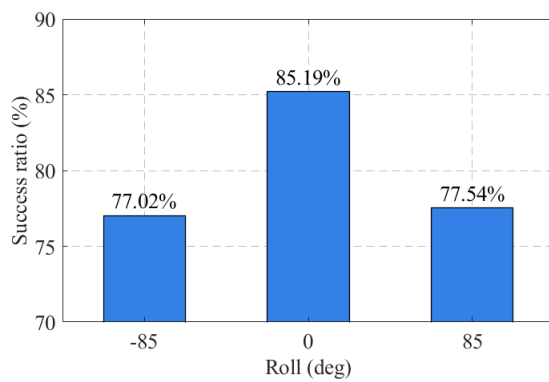


Fig. 19. Success ratio of the short distance policy with the initial distance of 8000 m and different initial roll conditions.

E. Training and validation of a small azimuth policy

According to the proposed multi-stage RL-based evasion strategy and the conditions and objectives determined

based on the analysis of the short distance policy in Section IV-D, a small azimuth policy is trained in this section. The small azimuth policy will be activated if the distance between the aircraft and the missile is larger than 8000 m and the magnitude of the azimuth of the missile is smaller than 30 deg. The objectives of small azimuth policy include (1) maintaining the magnitude of azimuth within 30 deg, (2) keeping the pitch and roll of the aircraft under control to avoid critical loss of altitude, (3) reducing the magnitude of the azimuth of the missile, and (4) accelerating the aircraft.

Training. According to the multi-stage RL-based evasion strategy and the objectives, the reward function of the small azimuth policy is defined as

$$r_{\text{small}} = r_{\text{small}}^{\text{roll}} + r_{\text{small}}^{\text{pitch}} + r_{\text{small}}^{\text{azimuth}} + r_{\text{small}}^{\text{vel}} + c_{\text{small}}^{\text{roll}} + c_{\text{small}}^{\text{pitch}} + c_{\text{small}}^{\text{azimuth}} + c_{\text{small}}^{\text{vel}} \quad (29)$$

where the reward terms are defined as

$$r_{\text{small}}^{\text{roll}} = 0.5e^{-\frac{|\phi|}{0.2}} \quad (30)$$

$$r_{\text{small}}^{\text{pitch}} = 0.5e^{-\frac{|\theta|}{0.2}} \quad (31)$$

$$r_{\text{small}}^{\text{azimuth}} = 1.0e^{-\frac{|\Psi|}{0.2}} \quad (32)$$

$$r_{\text{small}}^{\text{vel}} = 0.2 \tanh\left(\frac{\|\dot{x}_a\| - 350}{80}\right) \quad (33)$$

$$c_{\text{small}}^{\text{roll}} = \begin{cases} -20, & \text{if } |\phi| > 135 \text{ deg} \\ 0, & \text{otherwise} \end{cases} \quad (34)$$

$$c_{\text{small}}^{\text{pitch}} = \begin{cases} -20, & \text{if } |\theta| > 22.5 \text{ deg} \\ 0, & \text{otherwise} \end{cases} \quad (35)$$

$$c_{\text{small}}^{\text{azimuth}} = \begin{cases} -20, & \text{if } |\Psi| > 30 \text{ deg} \\ 0, & \text{otherwise} \end{cases} \quad (36)$$

$$c_{\text{small}}^{\text{vel}} = \begin{cases} -20, & \text{if } \|\dot{x}_a\| < 240 \text{ m/s or } \|\dot{x}_a\| > 510 \text{ m/s} \\ 0, & \text{otherwise} \end{cases} \quad (37)$$

To train a small azimuth policy, the initial velocity of the aircraft is divided into five intervals (i.e., 280 m/s to 320 m/s, 320 m/s to 360 m/s, 360 m/s to 400 m/s, 400 m/s to 440 m/s, and 440 m/s to 470 m/s) and the ratio of the possibility of selecting from the five intervals are 16, 8, 4, 2, and 1, respectively. If an interval is selected, then the initial velocity of the aircraft will be uniformly distributed in the interval. The training process initializes the other initial conditions of the aircraft in the same way as Section IV-C. The initial distance between the aircraft and the missile is divided into five intervals (i.e., 5000 m to 7000 m, 7000 m to 9000 m, 9000 m to 11000 m, 11000 m to 13000 m, and 13000 m to 15000 m) and the ratio of the possibility of selecting from the five intervals are 1, 2, 4, 8, and 16, respectively. The training process initializes the other initial conditions of the missile in the same way as Section IV-C. The maximum number of steps of an

episode is 7500. An episode will be terminated if the distance between the aircraft and the missile is less than 5000 m.

The learning process of the small azimuth policy can be reflected by the achieved reward presented in Fig. 20. The learning process converges in 6000 episodes.

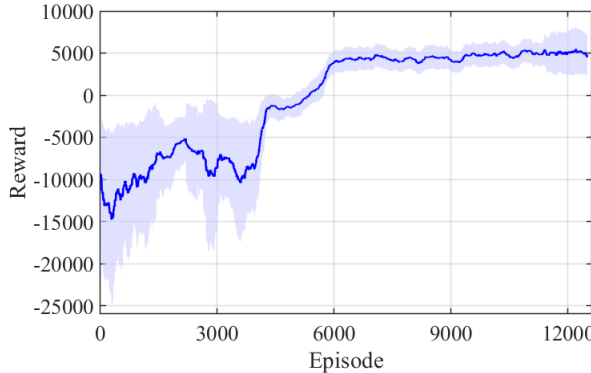


Fig. 20. Accumulated reward achieved in the training of the small azimuth policy.

Validation. To validate the small azimuth policy, a statistical analysis is conducted through dividing the initial conditions of the aircraft and the missile into intervals and then performing tests. The maximum number of steps of a test is 5000 (i.e., 25 s). (1) The initial velocity of the aircraft is divided into intervals ranging from 280 m/s to 470 m/s, with a step of 40 m/s. (2) The initial velocity of the missile is divided into intervals ranging from 800 m/s and 1400 m/s, with a step of 100 m/s. (3) The initial distance is set at 15000 m. (4) The initial azimuth of the missile is divided into intervals ranging from -30 deg to 30 deg, with a step of 12 deg. If an interval is selected, then the initial velocity of the aircraft, the initial velocity of the missile, and the initial azimuth of the missile will be uniformly distributed in the interval. The validation tests initialize the other initial conditions of the aircraft and the missile in the same way as Section IV-C.

For an interval determined by initial velocities of the aircraft and the missile, and the initial azimuth of the missile, the other initial conditions are randomly selected and one test have been conducted. The number of out-of-bounds occurrences for roll, pitch, velocity, and azimuth is listed in Table IV. The number of all out-of-bounds occurrences is zero, indicating that the constraint terms can effectively maintain the roll, pitch, velocity, and azimuth within corresponding defined ranges. For every interval, one representative test is randomly selected from the 30 tests. Fig. 21 and Fig. 22 show the average pitch and average roll of the aircraft in one episode according to the representative tests. It is shown that both average pitch and average roll are around 0 deg, indicating that the aircraft doesn't continuously perform aggress pitch or roll to climb, descend, or turn. Fig. 22 shows the

TABLE IV
Number of out-of-bounds occurrences for roll, pitch, velocity, and azimuth

Variable	Roll	Pitch	Velocity	Azimuth
Number of out-of-bounds	0	0	0	0

azimuth of the missile at the last step. With different initial conditions, the azimuth ranges from -3.5 deg to 3.5 deg, suggesting that the small azimuth policy has learned to reduce the azimuth of the missile. Fig. 24 shows the velocity increase ratio, indicating that the small azimuth policy can accelerate the aircraft.

The results indicate that the small azimuth policy can maintain the azimuth within 30 deg (Table IV) and keep the pitch and roll of the aircraft under control (Fig. 21 and Fig. 22). The small azimuth policy can reduce the magnitude of azimuth to around 3 deg or less (Fig. 22). The small azimuth policy can accelerate the aircraft also (Fig. 24). It is validated that the small azimuth policy can achieve the set objectives.

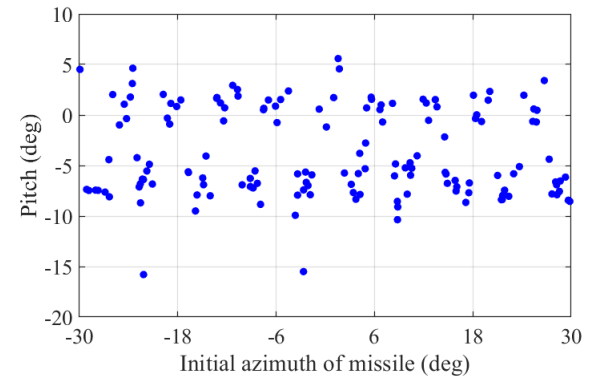


Fig. 21. Average pitch of the aircraft in a test following the small azimuth policy with different initial azimuth conditions.

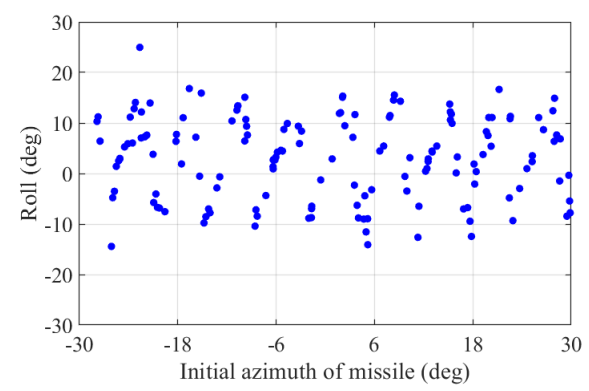


Fig. 22. Average roll of the aircraft in a test following the small azimuth policy with different initial azimuth conditions.

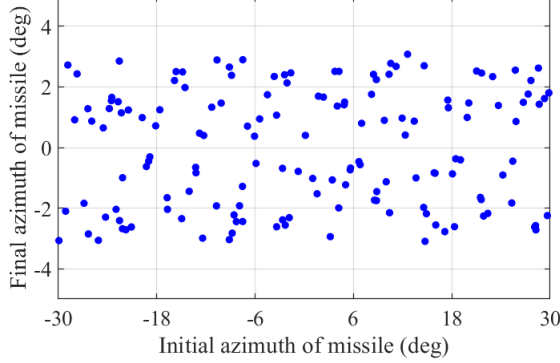


Fig. 23. Final azimuth of a test achieved by the small azimuth policy with different initial azimuth conditions.

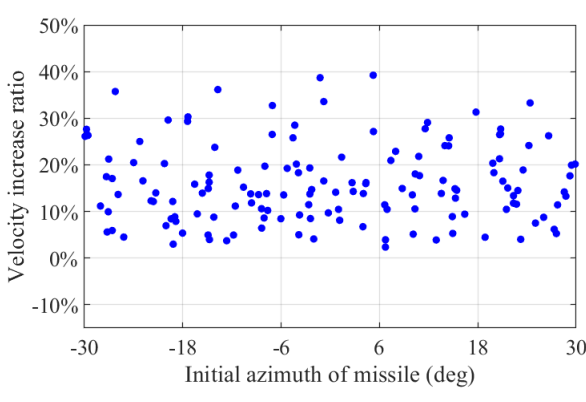


Fig. 24. Velocity increase rate of the final velocity to the initial velocity achieved by the small azimuth policy with different initial azimuth conditions.

F. Training and validation of a large azimuth policy

According to the proposed multi-stage RL-based evasion strategy and the conditions and objectives determined based on the analysis of the short distance policy in Section IV-D, a large azimuth policy is trained in this section. The large azimuth policy will be activated if the distance between the aircraft and the missile is larger than 8000 m and the magnitude of the azimuth of the missile is larger than 30 deg. The objectives of small azimuth policy include (1) reducing the azimuth of the missile, (2) reducing the magnitude of roll of the aircraft if the distance between the aircraft and the obstacle less than 8500 m to achieve a roll around 0 deg when switching to the short distance policy, (3) keeping the pitch of the aircraft under control, and (4) accelerating the aircraft.

Training. According to the multi-stage RL-based evasion strategy and the objectives, the reward function of the

large azimuth policy is defined as

$$r_{\text{large}} = r_{\text{large}}^{\text{roll}} + r_{\text{large}}^{\text{pitch}} + r_{\text{large}}^{\text{vel}} + c_{\text{large}}^{\text{roll}} + c_{\text{large}}^{\text{pitch}} + c_{\text{large}}^{\text{vel}} \quad (38)$$

It should be noted that the definition of $r_{\text{large}}^{\text{roll}}$ depends on the distance between the aircraft and the missile. $r_{\text{large}}^{\text{roll}}$ is defined as

$$r_{\text{large}}^{\text{roll}} = \begin{cases} r_{\text{large}}^{\text{far}}, & \|\Delta \mathbf{x}_m\| > 8500 \text{ m} \\ r_{\text{large}}^{\text{close}}, & \|\Delta \mathbf{x}_m\| \leq 8500 \text{ m} \end{cases} \quad (39)$$

If the distance between the aircraft and the missile is larger than the threshold (i.e., $\|\Delta \mathbf{x}_m\| > 8500$), the reward function is

$$r_{\text{large}}^{\text{far}} = 0.5e^{-\frac{|\phi - \text{sgn}((\Delta \mathbf{x}_m \times \dot{\mathbf{x}}_a) \cdot \mathbf{u}_{\text{up}}) \cdot 85|}{0.2}} \quad (40)$$

If the distance between the aircraft and the missile is smaller than the threshold (i.e., $\|\Delta \mathbf{x}_m\| \leq 8500$), the reward function is

$$r_{\text{large}}^{\text{close}} = \begin{cases} -20, & |\phi| > 30 \text{ deg} \\ 0.5, & |\phi| \leq 30 \text{ deg} \end{cases} \quad (41)$$

The other reward terms are defined as

$$r_{\text{large}}^{\text{pitch}} = 0.5e^{-\frac{|\theta|}{0.2}} \quad (42)$$

$$r_{\text{large}}^{\text{vel}} = 0.3 \tanh\left(\frac{\|\dot{\mathbf{x}}_a\| - 350}{60}\right) \quad (43)$$

$$c_{\text{large}}^{\text{roll}} = \begin{cases} -20, & \text{if } |\phi| > 135 \text{ deg} \\ 0, & \text{otherwise} \end{cases} \quad (44)$$

$$c_{\text{large}}^{\text{pitch}} = \begin{cases} -20, & \text{if } |\theta| > 22.5 \text{ deg} \\ 0, & \text{otherwise} \end{cases} \quad (45)$$

$$c_{\text{large}}^{\text{vel}} = \begin{cases} -20, & \text{if } \|\dot{\mathbf{x}}_a\| < 240 \text{ m/s or } \|\dot{\mathbf{x}}_a\| > 510 \text{ m/s} \\ 0, & \text{otherwise} \end{cases} \quad (46)$$

To train a small azimuth policy, the initial velocity of the aircraft is divided into five intervals (i.e., 280 m/s to 320 m/s, 320 m/s to 360 m/s, 360 m/s to 400 m/s, 400 m/s to 440 m/s, and 440 m/s to 470 m/s) and the ratio of the possibility of selecting from the five intervals are 16, 8, 4, 2, and 1, respectively. If an interval is selected, then the initial velocity of the aircraft will be uniformly distributed in the interval. The training process initializes the other initial conditions of the aircraft in the same way as Section IV-C. The initial distance between the aircraft and the missile is divided into five intervals (i.e., 5000 m to 7000 m, 7000 m to 9000 m, 9000 m to 11000 m, 11000 m to 13000 m, and 13000 m to 15000 m) and the ratio of the possibility of selecting from the five intervals are 1, 2, 4, 8, and 16, respectively. The initial azimuth of the missile is divided into ten intervals (i.e., 30 deg to 60 deg, 60 deg to 90 deg, 90 deg to 120 deg, 120 deg to 150 deg, 150 deg to 180 deg, -180 deg to -150 deg, -150 deg to -120 deg, -120 deg to -90 deg, -90 deg to -60 deg,

and -60 deg to -30 deg) and the ratio of the possibility of selecting from the ten intervals are 1, 2, 4, 8, 16, 16, 8, 4, 2, and 1, respectively. The training process initializes the other initial conditions of the missile in the same way as Section IV-C. The maximum number of steps of an episode is 7500. An episode will be terminated if the distance between the aircraft and the missile is less than 5000 m or the azimuth of the missile is large -15 deg and smaller than 15 deg.

The learning process of the large azimuth policy can be reflected by the achieved reward presented in Fig. 25. The learning process converges in 14000 episodes.

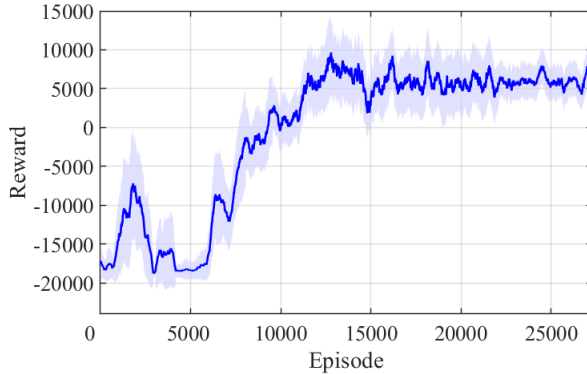


Fig. 25. Accumulated reward achieved in the training of the large azimuth policy.

Validation. To evaluate the large azimuth policy, a statistical analysis is conducted based on different initial conditions of the aircraft and the missile. The maximum number of steps of a test is 5000 (i.e., 25 s). (1) The initial velocity of the aircraft is set to 280 m/s. (2) The initial velocity of the missile is set to 800 m/s. (3) The initial distance is set at 15000 m. (4) The initial azimuth of the missile is set to -30 deg, -60 deg, -90 deg, -120 deg, -150 deg, 30 deg, 60 deg, 90 deg, 120 deg, 150 deg, and 180 deg, respectively. The validation tests initialize the other initial conditions of the aircraft and the missile in the same way as Section IV-C.

For an interval determined by initial velocities of the aircraft and the missile, and the initial azimuth of the missile, the other initial conditions are randomly selected and one test have been conducted. The number of out-of-bounds occurrences for roll, pitch, and velocity is listed in Table V. The number of all out-of-bounds occurrences is zero, indicating that the constraint terms can effectively maintain the roll, pitch, and velocity within corresponding defined ranges. Fig. 26 shows the change of azimuth achieved by the large azimuth policy and the steep turn policy with the same set of different initial directions. The large azimuth policy shows a turning capability comparable to the steep turn policy. Fig. 27 presents the roll of the aircraft at the last step of one episode. If the magnitude of the initial azimuth is small

TABLE V
Number of out-of-bounds occurrences for roll, pitch, and velocity

Variable	Roll	Pitch	Velocity
Number of out-of-bounds	0	0	0

(e.g., 30 deg and 60 deg), the large azimuth policy can turn the aircraft to achieve the termination condition - the magnitude of azimuth smaller than 15 deg, and the aircraft can terminate an episode by a large roll. If the magnitude of the initial azimuth is large, the large azimuth policy cannot finish a turn, and the large azimuth policy can reduce the roll of the aircraft to around 0 deg to achieve the beneficial roll condition of the short distance policy. Fig. 28 shows the average pitch of the aircraft in one episode. It is shown that the average pitch is around 0 deg, indicating that the aircraft doesn't continuously perform aggress pitch to climb or descend. Fig. 29 shows the velocity increase ratio, indicating that the large azimuth policy can accelerate the aircraft by about 10 percent.

The results indicate that the large azimuth policy can reduce the azimuth and has a performance comparable to the steep turn policy (Fig. 26). The large azimuth policy can reduce the magnitude of roll to around 0 deg if the distance reaches 8000 m (Fig. 27). The large azimuth policy can keep the pitch the aircraft under control (Fig. 28) and accelerate the aircraft (Fig. 29). It is validated that the large azimuth policy can achieve the set objectives.

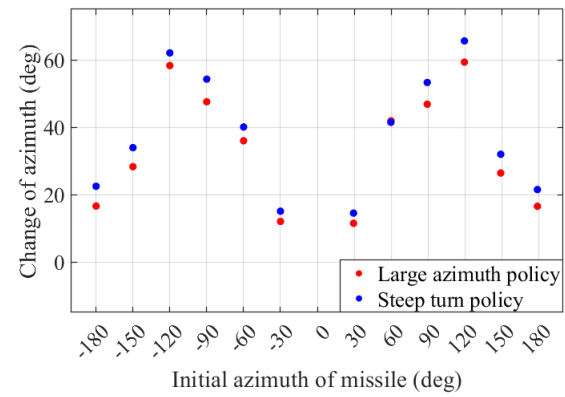


Fig. 26. Change of azimuth achieved by the large azimuth policy and the steep turn policy with different initial azimuth conditions.

G. Implementation of a baseline RL-based strategy

To evaluate the performance of the proposed multi-stage RL-based evasion strategy, this study compares the proposed multi-stage RL-based evasion strategy to an RL-based evasion strategy proposed in [1] and a steep turn strategy that is a classical evasion maneuver performed by human pilots [31]. Although scholars have proposed other RL-based evasion strategies, such as [4], [5], this study believe that the RL-based evasion strategy proposed

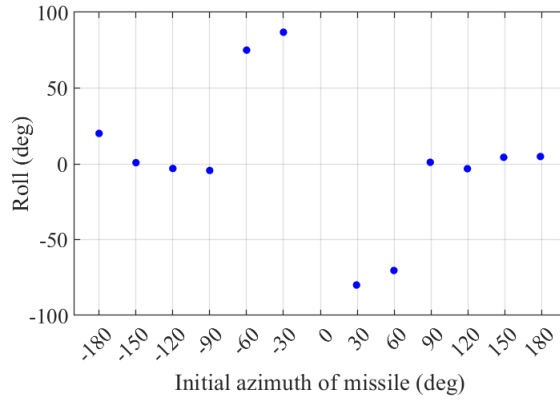


Fig. 27. Final roll of the aircraft following the large azimuth policy with different initial azimuth conditions.

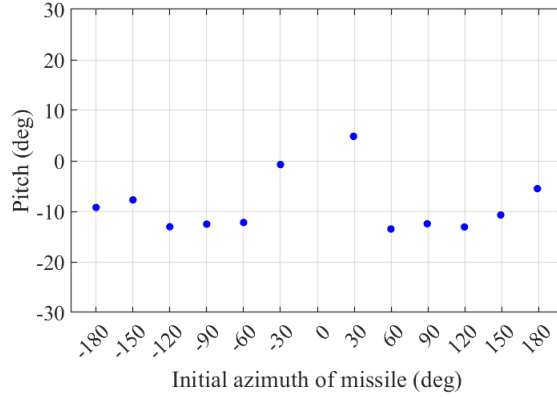


Fig. 28. Average pitch of the aircraft following the large azimuth policy with different initial azimuth conditions.

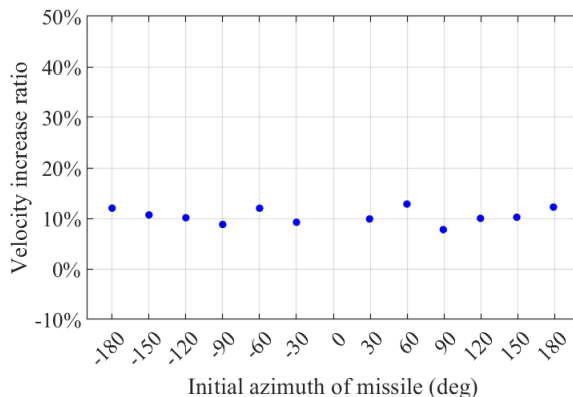


Fig. 29. Velocity increase rate of the final velocity to the initial velocity achieved by the large azimuth policy with different initial azimuth conditions.

in [1] is an appropriate baseline. Other RL-based evasion strategies may have one or more issues of lack of imple-

mentation details, considering issues additional to evasion (e.g., decoy), simple reward function, and obsolescence.

Training. In this section, an RL-based evasion policy is trained according to [1]. To ensure a fair comparison, for the training of a policy according to [1], the aircraft and the missile are initialized in the same way as the training of the short distance policy except that the missile is at a distance ranging from 5000 m to 15000 m from the aircraft. The policy uses the same state space and action space as the proposed multi-stage RL-based evasion strategy also.

Inspired by [1], the reward function of the baseline RL-based policy is defined as

$$r_{\text{baseline}} = r_{\text{baseline}}^{\text{distance}} + r_{\text{baseline}}^{\text{LOS}} + r_{\text{baseline}}^{\text{overload}} + r_{\text{baseline}}^{\text{pitch}} + r_{\text{baseline}}^{\text{roll}} \quad (47)$$

where $r_{\text{baseline}}^{\text{distance}}$ is a terminal reward related to distance and is defined as

$$r_{\text{baseline}}^{\text{distance}} = \begin{cases} -200(\min_1^T(\|\Delta\mathbf{x}_m(t)\|) - 10)^2, & \text{if, } \|\Delta\mathbf{x}_m(T)\| < 10 \text{ m} \\ 400(\min_1^T(\|\Delta\mathbf{x}_m(t)\|) - 10) + 4000, & \text{if } \|\Delta\mathbf{x}_m(T)\| \geq 10 \text{ m} \end{cases} \quad (48)$$

where T represents the number of steps of an episode. The LOS reward is defined as

$$r_{\text{baseline}}^{\text{LOS}} = 2.4 \ln(|\dot{\lambda}|) \quad (49)$$

Based on [1], the absolute LOS rate $|\dot{\lambda}|$ is calculated by

$$|\dot{\lambda}| = \frac{\|\mathbf{u}_m(t) - \mathbf{u}_m(t-1)\|}{\Delta t} \quad (50)$$

The overload reward is defined as

$$r_{\text{baseline}}^{\text{overload}} = -0.01n_m^2 \quad (51)$$

where n_m is the overload of the missile. It should be noted that the above-mentioned reward terms (48), (49), and (51) are proposed in [1]. To adapt the strategy to a three-dimensional scenario, the pitch reward and roll constraint of the short distance policy are applied to the baseline RL-based policy. The pitch reward aims to avoid severe loss of altitude, which is not a problem in the two-dimensional scenario discussed in [1]. The roll constraint prevents the aircraft rollover. The pitch reward and roll constraint are defined as

$$r_{\text{baseline}}^{\text{pitch}} = 0.5e^{-\frac{|\theta|}{0.2}} \quad (52)$$

$$r_{\text{baseline}}^{\text{roll}} = \begin{cases} -20, & \text{if } |\phi| > 135 \text{ deg} \\ 0, & \text{otherwise} \end{cases} \quad (53)$$

The maximum number of steps of an episode is 7500. If the distance between the aircraft and the missile is less than 10 m, the episode will not be terminated, aiming to record the minimum distance for achieved reward calculation.

The learning process of the baseline RL-based policy can be reflected by the achieved reward presented in Fig. 30. The learning process converges in 4500 episodes.

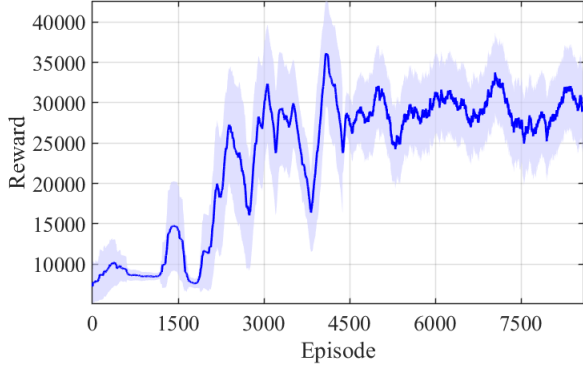


Fig. 30. Accumulated reward achieved by the training of the baseline RL-based evasion policy.

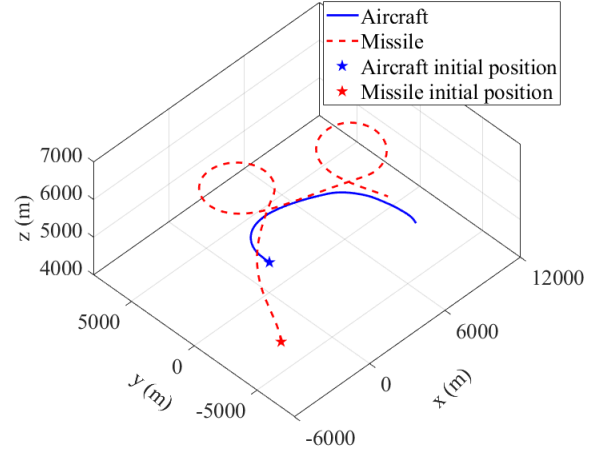


Fig. 31. Trajectory of the aircraft and the missile in the test of the baseline RL-based evasion policy.

Validation. To evaluate the performance of the baseline RL-based policy, a test is performed. The test has a maximum number of 5000 steps (i.e., 25 s). In the initial of the test, the position of the aircraft is set to [0, 0, 3970] (unit: m). The heading of the aircraft is set to 0 deg. Both the roll and pitch of the aircraft are set to 0 deg. The velocity of the aircraft is set to 280 m/s. The aircraft follows the baseline RL-based policy. The missile is 6000 m from the aircraft. The azimuth of the missile is -30 deg in a horizontal plane. The elevation of the missile is 10.72 deg. The velocity of the missile is 800 m/s. The maximum overload of the missile is randomly set to 40.53 g. The missile follows the PN law with a randomly selected navigation coefficient of 3.50.

Fig. 31 shows the trajectory of the aircraft and the missile. Fig. 32 shows the itemized accumulated rewards in one episode corresponding to distance, LOS rate, pitch, roll, and overload. It is shown that the baseline RL-based policy can balance the objectives in addressing the distance, LOS rate, and pitch, avoiding since the magnitude of the corresponding rewards is comparable, in avoiding large overload and roll loss of control. Fig. 33 shows the distance between the aircraft and the missile and the minimum distance used to calculate the distance reward is 20.37 m. Fig. 34, Fig. 35, Fig. 36, and Fig. 37 show the LOS rate, overload of the aircraft, pitch, and roll. One can see that the baseline RL-based policy can maintain the roll and pitch under control (Fig. 37 and Fig. 36) and considerably increase the LOS rate when the missile is close to the aircraft (Fig. 34). The overload of the aircraft is less than 6 g (Fig. 35), resulting from the overload reward that tends to attenuate the overload of the aircraft. It is shown that the baseline RL-based policy has learned to guide the aircraft to successfully avoid the missile (Fig. 31)

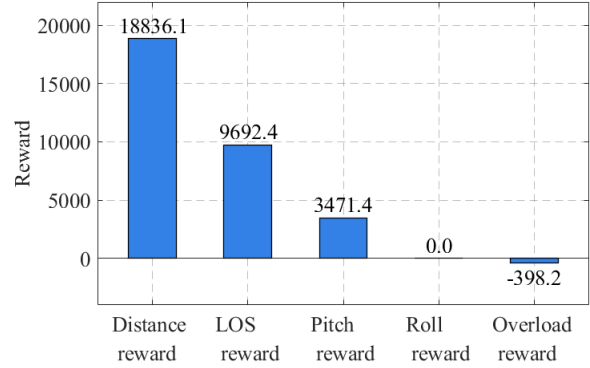


Fig. 32. Itemized accumulated rewards of an episode calculated based on the state of the aircraft and the missile in the test of the baseline RL-based evasion policy.

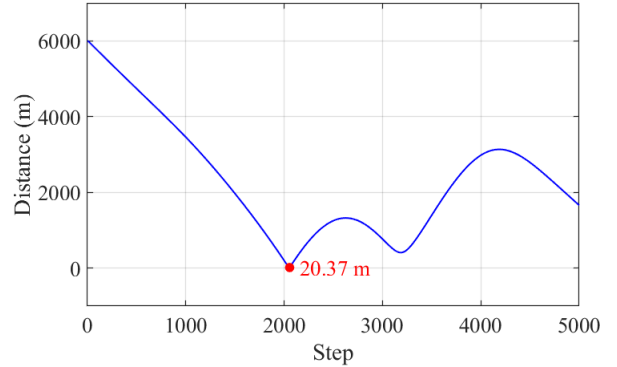


Fig. 33. Distance between the aircraft and the missile in the test of the baseline RL-based evasion policy.

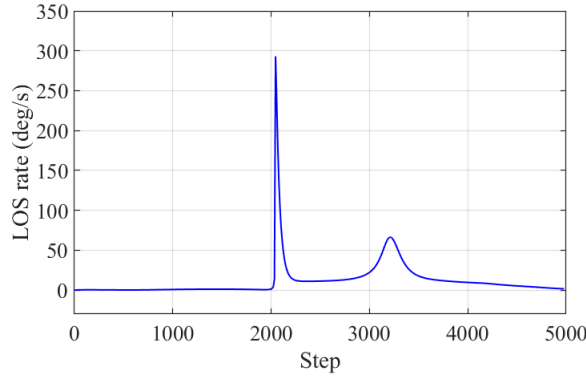


Fig. 34. LOS rate in the test of the baseline RL-based evasion policy.

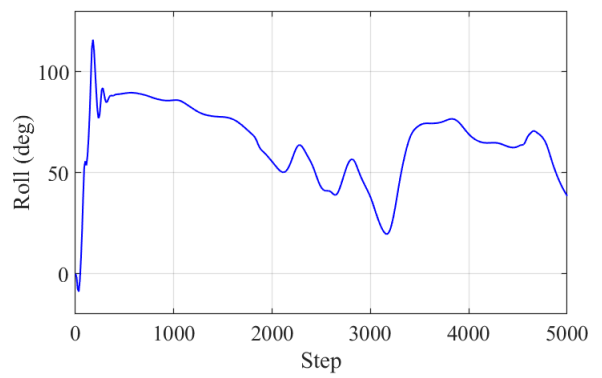


Fig. 37. Roll of the aircraft in the test of the baseline RL-based evasion policy.

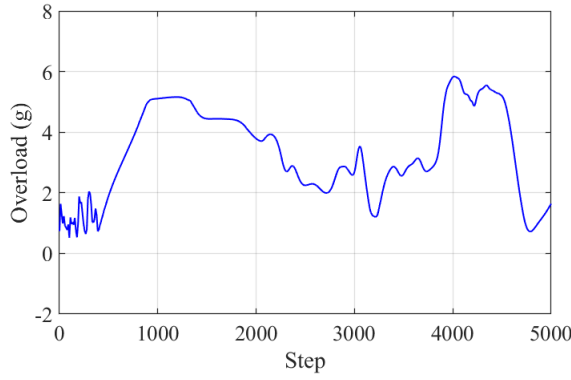


Fig. 35. Overload of the aircraft in the test of the baseline RL-based evasion policy.

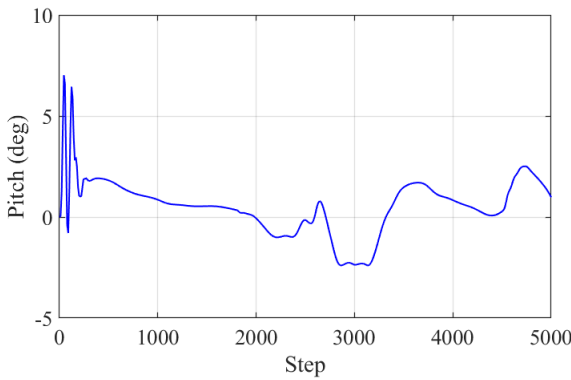


Fig. 36. Pitch of the aircraft in the test of the baseline RL-based evasion policy.

H. Comparison of the multi-stage RL-based strategy and baselines strategies

This section compares the proposed multi-stage RL-based evasion strategy to an RL-based evasion strategy

proposed in [1] and a steep turn strategy that is a classical evasion maneuver performed by human pilots [31], to evaluate the performance of the proposed strategy. The baseline RL-based evasion strategy is achieved in Section IV-G. The steep turn strategy is based on the steep turn policy is achieved in Section IV-C.

To investigate the three strategies, a statistical analysis is conducted through dividing the initial conditions of the aircraft and the missile into intervals and then performing tests. The maximum number of steps of a test is 5000 (i.e., 25 s). (1) The initial velocity of the aircraft is divided into intervals ranging from 280 m/s to 470 m/s, with a step of 40 m/s. (2) The initial velocity of the missile is divided into intervals ranging from 800 m/s and 1400 m/s, with a step of 100 m/s. (3) The initial distance between the aircraft and the missile is divided into intervals ranging from 5000 m to 15000 m, with a step of 1000 m. (4) The initial azimuth of the missile is divided into intervals ranging from -180 deg to 180 deg, with a step of 30 deg. The tests initialize the other initial conditions in the same way as the statistical analysis corresponding to Fig. 17.

For an interval determined by initial velocities of the aircraft and the missile, the initial distance between the aircraft and the missile, and the initial azimuth of the missile, the other initial conditions are randomly selected and 20 tests have been conducted for all three strategies. To ensure fairness in comparison, for the 20 tests, the aircraft addresses the same set of 20 scenarios determined according to the above-mentioned method, following the proposed strategy, traditional steep turn strategy, and baseline RL-based strategy, respectively. Fig. 38 presents the success ratio of the proposed multi-stage RL-based evasion strategy, baseline RL-based evasion strategy, and baseline steep turn evasion strategy. The proposed strategy achieves a success ratio of 80.89 percent in average, while the baseline RL-based strategy and the steep turn strategy achieve a success ratio of 34.14 percent and 3.34 percent in average, respectively, as shown in Table VI. It is validated that the proposed multi-stage RL-based

evasion strategy can guide the F-16 aircraft to avoid, at 80.89 percent probability, a missile with a random azimuth, a velocity of 800 m/s to 1400 m/s, a maximum overload of 40 g to 50 g, and a detection distance of 5000 m to 15000 m. If a missile is detected beyond 8000 m, the proposed strategy can achieve a success ratio of 85.06 percent in average. For every interval, one representative test is randomly selected from the 20 tests. Fig. 39 shows the maximum overload in one episode performed by the missile in chasing the aircraft with different evasion strategies, according to the representative tests. The proposed strategy can always force the missile to perform almost the maximum overload and the average maximum overload is 44.92 g. The baseline RL-based evasion strategy and steep turn evasion strategy cannot always force the missile to perform the maximum overload and the average maximum overload is 27.46 g and 16.27 g, respectively. The advantages of the proposed multi-stage RL-based evasion strategy in success ratio and in forcing the missile to perform maximum overload is validated.

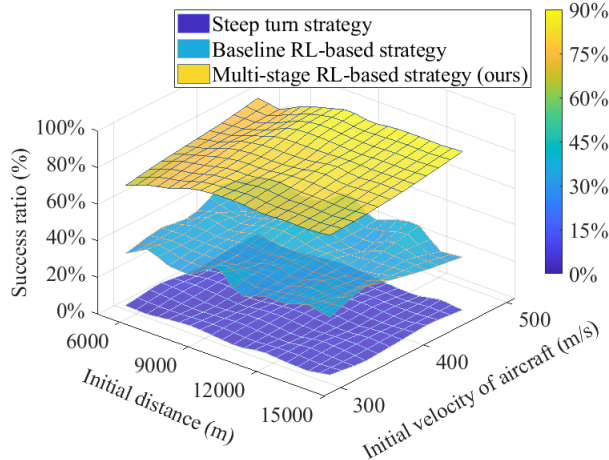


Fig. 38. Success ratio of the multi-stage RL-based evasion strategy, baseline RL-based evasion strategy, and baseline steep turn evasion strategy.

TABLE VI

Success ratio of the multi-stage RL-based evasion strategy, baseline RL-based evasion strategy, and baseline steep turn evasion strategy

Strategy	Multi-stage RL-based strategy	Baseline RL-based strategy	Steep turn strategy
Success ratio	80.89 %	34.14 %	3.34 %

I. Validation based on a missile with the augmented proportional navigation law

This study further evaluates the generalizability of the multi-stage RL-based strategy based on comparing

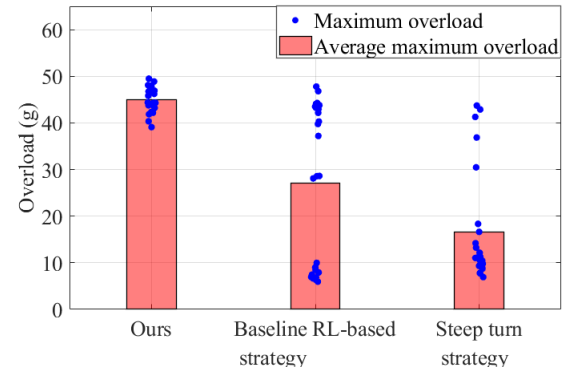


Fig. 39. Maximum overload performed by the missile to chase the aircraft with different strategies.

the performance of the strategy in addressing a missile with the APN law to the performance of the strategy in addressing a missile with the PN law. It should be noted that the multi-stage RL-based strategy has not been trained based on a missile with the APN law.

The APN law introduces an additional term that accounts for the acceleration of the aircraft to determine the missile command acceleration a_m and can be expressed as [47]

$$a_m = N \cdot V_c \cdot \dot{\lambda} + N' \cdot a_a^\perp \quad (54)$$

where a_a^\perp represents the perpendicular component of the aircraft's acceleration relative to the line of sight. N' is an aircraft acceleration correction coefficient. In the comparison, for a missile following the PN law, the navigation coefficient N is set randomly from 3 to 5. For a missile following the APN law, the navigation coefficient N is set randomly from 3 to 5 and the aircraft acceleration correction coefficient N' is randomly set from $0.5N$ to N according to [41]. The aircraft and the missile are initialized in the same way as the comparison of different strategies in Section IV-H. For an interval determined by the initial velocities of the aircraft and the missile, the initial distance between the aircraft and the missile, and the initial azimuth of the missile, the other initial conditions are randomly selected and 20 tests have been conducted for a missile with two different navigation laws. To ensure fairness in comparison, for the 20 tests, the aircraft addresses the same set of 20 scenarios determined according to the above-mentioned method.

The success ratio of the multi-stage RL-based evasion strategy in addressing a missile following the PN law and a missile following the APN law is presented in Fig. 40. Although the success ratio in addressing a missile following the APN law is lower than that in addressing a missile following the PN law, the success ratio in the former case can still reach 75.63 percent. The result is reasonable since APN law requires a higher initial acceleration command but the acceleration demand decreases at short distance, resulting in more overload available

to fight against the aggressive evasion maneuver of the aircraft [48]. The experimental results show that the multi-stage RL-based strategy is with certain generalizability to address different missiles that have not been involved in training.

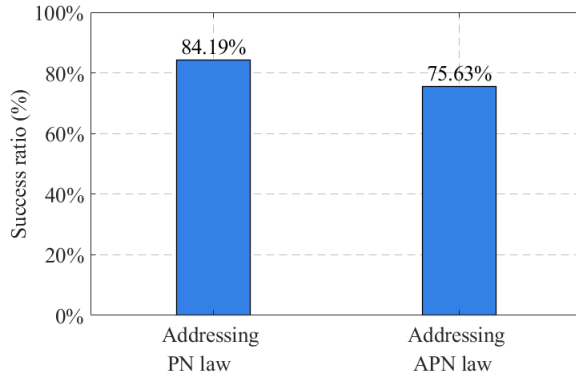


Fig. 40. Success ratio of the multi-stage RL-based evasion strategy in addressing a missile following different navigation laws.

V. Conclusion

This study developed a multi-stage RL-based strategy for aircraft to evade incoming missiles, particularly those detected at short range. The proposed strategy adopts a multi-stage architecture that learns a large-azimuth turning policy, a small-azimuth escape policy, and a short-range aggressive maneuver policy. At each stage, one of the three policies is activated based on distance and azimuth.

The proposed multi-stage RL-based strategy, a baseline RL-based strategy, and a conventional steep-turn strategy were evaluated against missiles under various conditions in a high-fidelity simulation environment modeling an F-16 aircraft and a missile. Experimental results show that the proposed method achieves superior performance, enabling the F-16 aircraft to avoid missiles with a probability of 80.89 percent for velocities ranging from 800 m/s to 1400 m/s, maximum overloads from 40 g to 50 g, detection distances from 5000 m to 15000 m, and random azimuths. When the missile is detected beyond 8000 m, the success ratio increases to 85.06 percent. In comparison, the baseline RL-based and steep-turn strategies achieved success ratios of only 34.14 percent and 3.34 percent, respectively. The statistical analysis indicates that the machine-learning-based multi-stage strategy can significantly strengthen the final line of defense for aircraft in modern air combat.

REFERENCES

[1] T. Yan, C. Liu, M. Gao, Z. Jiang, and T. Li, “A Deep Reinforcement Learning-Based Intelligent Maneuvering Strategy for the High-Speed UAV Pursuit-Evasion Game,” *Drones*, vol. 8, no. 7, 2024.

[2] Y. Wang, J. Wang, and S. Fan, “Parameter Identification of a PN-Guided Incoming Missile Using an Improved Multiple-Model Mechanism,” *IEEE Transactions on Aerospace and Electronic Systems*, vol. 59, no. 5, pp. 5888–5899, 2023.

[3] Z. Tian, M. Danino, Y. Bar-Shalom, and B. Milgrom, “Aircraft Defense With Jamming Against a Pursuer With Limited Field-of-View,” *IEEE Transactions on Aerospace and Electronic Systems*, vol. 61, no. 5, pp. 14479–14489, 2025.

[4] A. Cook, V. Gavra, J. Haindl, S. Neumeier, A. Perez-Acal, and J. R. de Amaral, “Missile Avoidance using Reinforcement Learning,” *AIAA Science and Technology Forum and Exposition, AIAA SciTech Forum 2025*, no. January, pp. 1–19, 2025.

[5] C. Zhang, J. Song, C. Tao, Z. Su, Z. Xu, W. Feng, Z. Zhang, and Y. Xu, “Adaptive Missile Avoidance Algorithm for UAV Based on Multi-Head Attention Mechanism and Dual Population Confrontation Game,” *Drones*, vol. 9, no. 5, 2025.

[6] X. Gong, W. Chen, Z. Chen, and W. Yuan, “Closed-Form Solutions of Miss Distance for Higher-Order Guidance System,” *IEEE Transactions on Aerospace and Electronic Systems*, vol. 60, no. 2, pp. 2331–2349, 2024.

[7] C. Peng, H. Zhang, Y. He, and J. Ma, “State-Following-Kernel-Based Online Reinforcement Learning Guidance Law Against Maneuvering Target,” *IEEE Transactions on Aerospace and Electronic Systems*, vol. 58, no. 6, pp. 5784–5797, 2022.

[8] Z. Tian, M. Danino, Y. Bar-Shalom, and B. Milgrom, “Missile Threat Detection and Evasion Maneuvers With Countermeasures for a Low-Altitude Aircraft,” *IEEE Transactions on Aerospace and Electronic Systems*, pp. 1–23, 2023.

[9] V. N. Evdokimenkov, D. A. Kozorez, and L. N. Rabinskiy, “Unmanned aerial vehicle evasion manoeuvres from enemy aircraft attack,” *Journal of the Mechanical Behavior of Materials*, vol. 30, no. 1, pp. 87–94, 2021.

[10] Z. Tian, M. Danino, Y. Bar-Shalom, and B. Milgrom, “Estimation-based missile threat detection and evasion maneuver for a low-altitude aircraft,” in *Proc. SPIE*, vol. 12547, 6 2023, p. 1254704.

[11] Q. Du, Y. Hu, W. Jing, and C. Gao, “Three-dimensional target evasion strategy without missile guidance information,” *Aerospace Science and Technology*, vol. 157, p. 109857, 2025.

[12] Y. Ou, H. Xiong, H. Jiang, Y. Zhang, and B. R. Noack, “Dynamic Obstacle Avoidance of Fixed-wing Aircraft in Final Phase via Reinforcement Learning,” *IEEE Transactions on Aerospace and Electronic Systems*, pp. 1–14, 2024.

[13] S. G. Clarke and I. Hwang, “Deep reinforcement learning control for aerobatic maneuvering of agile fixed-wing aircraft,” in *AIAA Scitech 2020 Forum*, 2020, pp. 1–18.

[14] Q. Qu, K. Liu, W. Wang, and J. Lu, “Spacecraft Proximity Maneuvering and Rendezvous With Collision Avoidance Based on Reinforcement Learning,” *IEEE Transactions on Aerospace and Electronic Systems*, 2022.

[15] H. Jiang, H. Xiong, W. Zeng, and Y. Ou, “Safely Learn to Fly Aircraft From Human: An Offline-Online Reinforcement Learning Strategy and Its Application to Aircraft Stall Recovery,” *IEEE Transactions on Aerospace and Electronic Systems*, vol. 59, no. 6, pp. 8194–8207, 2023.

[16] J. Chai, W. Chen, Y. Zhu, Z. X. Yao, and D. Zhao, “A Hierarchical Deep Reinforcement Learning Framework for 6-DOF UCAV Air-to-Air Combat,” *IEEE Transactions on Systems, Man, and Cybernetics: Systems*, vol. 53, no. 9, pp. 5417–5429, 2023.

[17] W. Wang, L. Ru, M. Lv, and L. Mo, “Dynamic and adaptive learning for autonomous decision-making in beyond visual range air combat,” *Aerospace Science and Technology*, vol. 163, p. 110327, 2025.

[18] A. P. Pope, J. S. Ide, D. Mićović, H. Diaz, J. C. Twedt, K. Alcedo, T. T. Walker, D. Rosenbluth, L. Ritholtz, and D. Javorsek, “Hierarchical Reinforcement Learning for Air Combat at DARPA’s AlphaDogfight Trials,” *IEEE Transactions on Artificial Intelligence*, vol. 4, no. 6, pp. 1371–1385, 2023.

[19] X. Ma, Y. Yuan, and L. Guo, "Hierarchical Reinforcement Learning for UAV-PE Game With Alternative Delay Update Method," *IEEE Transactions on Neural Networks and Learning Systems*, vol. 36, no. 3, pp. 4639–4651, 2025.

[20] J. Bertram and P. Wei, "An Efficient Algorithm for Multiple-Pursuer-Multiple-Evader Pursuit/Evasion Game," in *AIAA Scitech 2021 Forum*, ser. AIAA SciTech Forum. American Institute of Aeronautics and Astronautics, 1 2021.

[21] M. Gao, T. Yan, Q. Li, W. Fu, and J. Zhang, "Intelligent Pursuit–Evasion Game Based on Deep Reinforcement Learning for Hypersonic Vehicles," *Aerospace*, vol. 10, no. 1, 2023.

[22] Z. Li, J. Wu, Y. Wu, Y. Zheng, M. Li, and H. Liang, "Real-time Guidance Strategy for Active Defense Aircraft via Deep Reinforcement Learning," in *IEEE National Aerospace and Electronics Conference*, 2021, pp. 177–183.

[23] C. Liu, L. Dou, R. Zhang, Y. Tang, M. Ren, and L. Zhang, "PITD3-based Autonomous Evasion Decision-making Method for Aircraft," in *2024 43rd Chinese Control Conference (CCC)*, 2024, pp. 8606–8611.

[24] K. Chen, J. Lei, and B. Li, "The Pursuit-Evasion Game Strategy of High-Speed Aircraft Based on Monte-Carlo Deep Reinforcement Learning," in *2021 5th Chinese Conference on Swarm Intelligence and Cooperative Control*, Z. Ren, M. Wang, and Y. Hua, Eds. Singapore: Springer Nature Singapore, 2023, pp. 1616–1627.

[25] E. Scukins, M. Klein, L. Kroon, and P. Ögren, "Deep Learning Based Situation Awareness for Multiple Missiles Evasion," in *2024 International Conference on Unmanned Aircraft Systems (ICUAS)*, 2024, pp. 1446–1452.

[26] K. Chen, J. Lei, and B. Li, "The Research on Evasion Strategy of Unpowered Aircraft Based on Deep Reinforcement Learning," *Journal of Physics: Conference Series*, vol. 2252, no. 1, p. 12072, 2022.

[27] M. M. Özbek and E. Koyuncu, "Missile Evasion Maneuver Generation with Model-free Deep Reinforcement Learning," in *International Conference on Recent Advances in Air and Space Technologies (RAST)*, 2023, pp. 1–6.

[28] Y. Li, L. Zhang, K. Wang, F. Zhang, and Y. Fan, "Research on Evasion Strategy of Aircraft Based on Deep Reinforcement Learning," in *Lecture Notes in Electrical Engineering*, vol. 833 LNEE, 2022, pp. 653–665.

[29] Y. Yuan, J. Yang, Z. L. Yu, Y. Cheng, P. Jiao, and L. Hua, "Hierarchical Goal-Guided Learning for the Evasive Maneuver of Fixed-Wing UAVs based on Deep Reinforcement Learning," *Journal of Intelligent & Robotic Systems*, vol. 109, no. 2, p. 43, 2023.

[30] C. Xiao, P. Lu, and Q. He, "Flying Through a Narrow Gap Using End-to-End Deep Reinforcement Learning Augmented With Curriculum Learning and Sim2Real," *IEEE Transactions on Neural Networks and Learning Systems*, pp. 1–8, 2021.

[31] X. Yang and J. Ai, "Evasive Maneuvers Against Missiles for Unmanned Combat Aerial Vehicle in Autonomous Air Combat," *Xi Tong Fangzhen Xuebao / Journal of System Simulation*, vol. 30, no. 5, pp. 1957–1966, 2018.

[32] B. Li, Y. Wu, and G. Li, "Hierarchical reinforcement learning guidance with threat avoidance," *Journal of Systems Engineering and Electronics*, vol. 33, no. 5, pp. 1173–1185, 2022.

[33] J. Berndt, "JSBSim: An Open Source Flight Dynamics Model in C++," in *AIAA Modeling and Simulation Technologies Conference and Exhibit*, ser. Guidance, Navigation, and Control and Co-located Conferences. American Institute of Aeronautics and Astronautics, 8 2004.

[34] Z. Zhou, J. Jiang, H. Wang, X. Wu, W. Deng, and X. Chen, "Enhancing Proximal Policy Optimization for UAV Air Combat with Exploration Boosting and Covariance Matrix Adaptation Strategy," *IEEE Access*, p. 1, 2025.

[35] I. Moran and T. Altilar, "Three plane approach for 3D true proportional navigation," in *AIAA guidance, navigation, and control conference and exhibit*, 2005, p. 6457.

[36] Z. Yang, D. Zhou, W. Kong, H. Piao, K. Zhang, and Y. Zhao, "Non-dominated Maneuver Strategy Set With Tactical Requirements for a Fighter Against Missiles in a Dogfight," *IEEE Access*, vol. 8, pp. 117298–117312, 2020.

[37] P. Geuzaine, G. Brown, C. Harris, and C. Farhat, "Aeroelastic Dynamic Analysis of a Full F-16 Configuration for Various Flight Conditions," *AIAA Journal*, vol. 41, no. 3, pp. 363–371, 3 2003.

[38] D. Hu, R. Yang, J. Zuo, Z. Zhang, J. Wu, and Y. Wang, "Application of deep reinforcement learning in maneuver planning of beyond-visual-range air combat," *IEEE Access*, vol. 9, pp. 32282–32297, 2021.

[39] W.-r. Kong, D.-y. Zhou, Y.-j. Du, Y. Zhou, and Y.-y. Zhao, "Hierarchical multi-agent reinforcement learning for multi-aircraft close-range air combat," *IET Control Theory & Applications*, vol. 17, no. 13, pp. 1840–1862, 9 2023.

[40] M. Yan, R. Yang, Y. Zhang, L. Yue, and D. Hu, "A hierarchical reinforcement learning method for missile evasion and guidance," *Scientific Reports*, vol. 12, no. 1, pp. 1–21, 2022.

[41] Y. Alqudsi and G. El-Bayoumi, "A qualitative comparison between the proportional navigation and differential geometry guidance algorithms," *INCAS Bulletin*, vol. 10, no. 2, 2018.

[42] Z. Yang, D. Zhou, Y. Zhao, W. Kong, K. Zhang, and L. Zeng, "Tactical preference based objectives for solving an evasion problem of fighter in air combat," *Journal of Physics: Conference Series*, vol. 1570, no. 1, p. 12024, 2020.

[43] F. Neele, "Two-color infrared missile warning sensors," in *Airborne Intelligence, Surveillance, Reconnaissance (ISR) Systems and Applications II*, vol. 5787. SPIE, 2005, pp. 134–145.

[44] B. Zhao, Q. Zhang, X. Huang, T. Han, and J. Chen, "Deep Reinforcement Learning Proportional Navigation Guidance Law Against High-Speed Maneuvering Targets Considering Field-of-View Limit," *IEEE Transactions on Aerospace and Electronic Systems*, pp. 1–15, 2025.

[45] X. Wang, M. Yang, S. Wang, M. Hou, and T. Chao, "Linear-quadratic and norm-bounded combined differential game guidance scheme with obstacle avoidance for attacking defended aircraft in three-player engagement," *Defence Technology*, vol. 42, pp. 136–155, 2024.

[46] F. Tyan, "Analysis of 3D PPN guidance laws for nonmaneuvering target," *IEEE Transactions on Aerospace and Electronic Systems*, vol. 51, no. 4, pp. 2932–2943, 2015.

[47] Y. B. Shtessel, I. A. Shkolnikov, and A. Levant, "Smooth second-order sliding modes: Missile guidance application," *Automatica*, vol. 43, no. 8, pp. 1470–1476, 2007.

[48] Y. Liu, K. Li, L. Chen, and Y. Liang, "Novel augmented proportional navigation guidance law for mid-range autonomous rendezvous," *Acta Astronautica*, vol. 162, pp. 526–535, 2019.